Threshold Dynamics and Bifurcation of a State-Dependent Feedback Nonlinear Control Susceptible–Infected–Recovered Model[1]

Tianyu Cheng
School of Mathematics and Information Science,
Shaanxi Normal University,
Xi'an 710119, China

Sanyi Tang[2]
School of Mathematics and Information Science,
Shaanxi Normal University,
Xi'an 710119, China
e-mails: sytang@snnu.edu.cn;
sanyitang219@hotmail.com

Robert A. Cheke
Natural Resources Institute,
University of Greenwich at Medway,
Central Avenue, Chatham Maritime,
Chatham, Kent ME4 4TB, UK

A classic susceptible–infected–recovered (SIR) model with nonlinear state-dependent feedback control is proposed and investigated in which integrated control measures, including vaccination, treatment and isolation, are applied once the number of the susceptible population reaches a threshold level. The interventions are density dependent due to limitations on the availability of resources. The existence and global stability of the disease-free periodic solution (DFPS) are addressed, and the threshold condition is provided, which can be used to define the control reproduction number R_c for the model with state-dependent feedback control. The DFPS may also be globally stable even if the basic reproduction number R_0 of the SIR model is larger than one. To show that the threshold dynamics are determined by the R_c, we employ bifurcation theories of the discrete one-parameter family of maps, which are determined by the Poincaré map of the proposed model, and the main results indicate that under certain conditions, a stable or unstable interior periodic solution could be generated through transcritical, pitchfork, and backward bifurcations. A biphasic vaccination rate (or threshold level) could result in an inverted U-shape (or U-shape) curve, which reveals some important issues related to disease control and vaccine design in bioengineering including vaccine coverage, efficiency, and vaccine production. Moreover, the nonlinear state-dependent feedback control could result in novel dynamics including various bifurcations. [DOI: 10.1115/1.4043001]

Keywords: SIR model, disease free periodic solution, control reproduction number, Poincaré map, transcritical and pitchfork bifurcations, backward bifurcation

1 Introduction

Although outbreaks of traditional infectious diseases have been prevented or controlled in the recent past, outbreaks of emerging infectious diseases such as SARS, H1N1 influenza, Dengue fever, and Ebola, have provided new threats and challenges. Comprehensive prevention and control strategies, including quarantine, isolation, vaccination, and treatment, are widely used to reduce the spread of such infectious diseases [1–4] but evaluating the effectiveness of the mitigating measures is also crucial. To address this problem, mathematical models can play key roles by modeling the control tactics and revealing their effectiveness.

Recently, several mathematical models have been proposed to investigate integrated control impacts [3,4]. Existing approaches to modeling the impact of integrated control measures have focused on how to include the tactics into models and address their effects on the dynamics and disease control. There are two types of important models to be chosen according to how the control measures are implemented: continuous models with a continuous control strategy [1–4] and continuous models with a discrete (pulse) control strategy [5–7]. The two types of models with the continuous vaccination and pulsed vaccination were compared with each other in epidemiological models [5]. The results of that study were confirmed by the pulse vaccination campaigns against measles performed in 1994 in the United Kingdom, which revealed that a pulse vaccination strategy had a dramatic impact on the development of the epidemic.

Applying the impulse vaccination strategy at a fixed period T means vaccinating a proportion of the susceptible population at discrete time points $nT(n = 1,2,\ldots)$ and removing into the recovered or vaccinated class instantaneously. This type of strategy can be formulated by impulse differential equation with a fixed time moment [7–14]. The dynamical behavior, including the existence and local stability of the disease-free periodic solution (DFPS), has been investigated, which revealed that pulse vaccination was always capable of eradicating the diseases, usually doing better than continuous vaccination. Numerical bifurcation analyses depict that pulse vaccination can lead to very complex dynamics including chaotic behavior. In addition, this type of modeling has been widely used for cancer treatment [15–19] and HIV control [20,21].

However, one common assumption of all the above models is that, regardless of the size of the susceptible population, the pulse vaccination control is implemented at fixed periods. The obvious conclusion is that as long as the pulse period is small enough, the disease can be controlled and eradicated eventually. Moreover, from a mathematical point of view, fixed moment control will result in a nonautonomous system, which poses a considerable challenge to theoretical analysis. In particular, it is difficult to define the control reproduction number R_c and investigate the threshold dynamics of the proposed models [7,8,11–14]. In order to overcome the above shortcomings, a different modeling method is proposed in the present paper, i.e., we consider whether or not the integrated control strategy is implemented depends on the number in the susceptible population rather than having it applied at a fixed period. This can be modeled by state-dependent impulsive differential equations (so-called impulsive semidynamical systems) [22–31]. Recently, impulsive semidynamical systems have been widely used to model biological systems with threshold control strategies, such as biological resource and pest

[1]Fully documented templates are available in the elsarticle package on CTAN.
[2]Corresponding author.

Contributed by the Design Engineering Division of ASME for publication in the Journal of Computational and Nonlinear Dynamics. Manuscript received December 10, 2018; final manuscript received February 25, 2019; published online April 8, 2019. Assoc. Editor: Xiaopeng Zhao.

management programs, and chemostat cultures in ecological systems [27,28,32–37].

Therefore, in the present paper, we extend the classic susceptible–infected–recovered (SIR) infectious model with a state-dependent feedback control strategy. In particular, although state- dependent impulsive models triggered by the infectious population size are reasonable, such models do not have a feasible disease-free equilibrium nor can the disease be completely eradicated, so far as mathematical and epidemiological points of view are concerned. Therefore, the time when vaccination strategies are implemented should, perhaps, be dependent on the level of susceptibility instead of disease infection rates. So, in this study, we propose a state-dependent impulsive model describing susceptible population-triggered vaccination and isolation incorporating continuous treatment for the patients. We assume that there exists a threshold level S_v for the susceptible population such that integrated control measures (pulse vaccination, treatment, or isolation strategies) are implemented once the susceptible population number reaches S_v. Furthermore, the numbers in the susceptible and infected populations that are vaccinated and treated (or isolated), respectively, depend on their densities. This indicates that the pulse controls are nonlinear due to limitations on the amount of resources available. Note that linear pulse control has been addressed in Ref. [38], from which the existence and stability of a disease-free periodic solution were studied, and the bifurcations related to the key parameters were also investigated.

The main purpose of this study is to develop analytical techniques and provide a comprehensive qualitative analysis of the global dynamics by analyzing a planar impulsive SIR semidynamic model, and to address the effects of nonlinear feedback pulse control on the dynamics including the bifurcations in comparison with the results obtained in Ref. [38]. To achieve these aims, the existence and global stability of the DFPS, which corresponds to the disease free equilibrium, are first addressed. The control reproduction number R_c for the model with state-dependent feedback control can be defined by the Floquet multiplier, which ensures the local stability of the DFPS. It is interesting that the DFPS may also be globally stable even if the basic reproduction number R_0 of the classic SIR model is larger than one. In order to depict the threshold dynamics determined by the R_c, we employ the bifurcation theories of the discrete one-parameter family of maps, which is determined by the Poincaré map of the planar impulsive SIR semidynamic model. We choose the maximal vaccination rate, maximal treatment rate or isolation rate, threshold level S_v, and birth rate of the susceptible population to reveal transcritical and pitchfork bifurcations, which can depict the threshold dynamics completely. The main bifurcation results indicate that under certain conditions a stable or an unstable interior periodic solution could be generated through transcritical and pitchfork bifurcations. In particular, the stable DFPS and the interior equilibrium of the SIR model can coexist once an unstable interior periodic solution has bifurcated ($R_c < 1 < R_0$ here), i.e., backward bifurcation occurs. Furthermore, we discuss the corresponding biological implications related to the disease control and vaccine design in bioengineering.

2 The Model

Let $S(t)$, $I(t)$, and $R(t)$ be the densities of susceptible, infected, and removed parts of the population at time t, respectively, and then $N(t) = S(t) + I(t) + R(t)$ denotes the total population. Without loss of generality, we may assume that the total population $N(t)$ is a constant or tends to a constant as t approaches infinity. Therefore, for the classical SIR model, we only need to consider the following two-dimensional system:

$$\begin{cases} \dfrac{dS(t)}{dt} = \Lambda - \beta SI - \delta S \\ \dfrac{dI(t)}{dt} = \beta SI - qI \end{cases} \tag{1}$$

where Λ denotes the birth rate, δ is the death rate, γ represents the recovery rate with $q = \gamma + \delta$, and β denotes the transmission rate.

It is easy to know that the region

$$D = \{(S, I) | S \geq 0, I \geq 0, S + I \leq \Lambda/\delta\}$$

is an invariant set of model (1). Solving $\Lambda - \beta SI - \delta S = 0$ and $\beta SI - qI = 0$ with respect to I yields two isolines as follows:

$$l_1 : S = \frac{q}{\beta}, \quad l_2 : I = \frac{-\delta S + \Lambda}{\beta S} \doteq h(S)$$

where $\doteq$ means definition in this paper.

By defining $R_0 = \Lambda\beta/\delta q$, we have the following results for model (1), which are useful for the coming qualitative analyses [38].

Lemma 1. *If $R_0 \leq 1$, then model (1) has a disease-free equilibrium $(K, 0)$ with $K = \Lambda/\delta$, which is a globally stable node; if $R_0 > 1$, then there exists a unique interior equilibrium (S^*, I^*) with $S^* = q/\beta$, $I^* = \Lambda\beta - \delta q/\beta q$, which is a globally stable node (when $\Delta \geq 0$) or focus (when $\Delta < 0$). Further, if $R_0 \in (1, R_1] \cup [R_2, +\infty)$, then the unique endemic equilibrium $P^*(S^*, I^*)$ is a globally stable node; if $R_0 \in (R_1, R_2)$, then $P^*(S^*, I^*)$ is a globally stable focus, where $\Delta = \delta^2 R_0^2 - 4\delta q R_0 + 4\delta q$, $R_1 = 2(\delta + \gamma - \sqrt{\gamma(\delta + \gamma)})/\delta$, $R_2 = 2(\delta + \gamma + \sqrt{\gamma(\delta + \gamma)})/\delta$ and $R_2 > 2 > R_1 > 1$.*

2.1 The Susceptible–Infected–Recovered Model With State-Dependent Feedback Nonlinear Control. In order to consider the saturation phenomenon resulting from the limited resources, we fix the two impulsive functions to be nonlinear continuously differentiable functions $[1 - \eta_1 S(t)/S(t) + h_1]S(t)$ and $[1 - \eta_2 I(t)/I(t) + h_2]I(t)$. Here, $1 > \eta_1 \geq 0$ represents the maximal vaccination rate and $h_1 \geq 0$ denotes the half saturation constant for the susceptible population. $1 > \eta_2 \geq 0$ represents the maximal treatment or isolation rate and $h_2 \geq 0$ denotes the half saturation constant for the infected population. We assume that the initial density of the susceptible population is less than the threshold vaccination level S_v and the integrated mitigating measures including vaccination, treatment, and isolation are conducted once the density of the susceptible population reaches the threshold S_v, when the densities of both the susceptible and infected populations are updated to $[1 - \eta_1 S_v/S_v + h_1]S_v$ and $[1 - \eta_2 I(t)/I(t) + h_2]I(t)$, respectively.

Based on the above, we propose the following SIR model with state-dependent feedback nonlinear control:

$$\begin{cases} \left.\begin{aligned} \dfrac{dS(t)}{dt} &= \Lambda - \beta SI - \delta S, \\ \dfrac{dI(t)}{dt} &= \beta SI - \gamma I - \delta I, \end{aligned}\right\} & S(t) < S_v \\ \left.\begin{aligned} S(t^+) &= \left[1 - \dfrac{\eta_1 S(t)}{S(t) + h_1}\right] S(t), \\ I(t^+) &= \left[1 - \dfrac{\eta_2 I(t)}{I(t) + h_2}\right] I(t), \end{aligned}\right\} & S(t) = S_v \end{cases} \tag{2}$$

Denoting the following functions $B_1(S) = -\eta_1 S^2/S + h_1$, $B_2(I) = -\eta_2 I^2/I + h_2$ and $f(I) = I + B_2(I) < I$, then by simple calculations, we have:

$$B_2'(I) = -\frac{\eta_2 I(I + 2h_2)}{(I + h_2)^2}, f'(I) = \frac{(1 - \eta_2)I^2 + 2h_2(1 - \eta_2)I + h_2^2}{(I + h_2)^2}$$

It is easy to see that $f'(I) > 0$ for all $I > 0$, which indicates that $f(I)$ is a monotonically increasing function.

To prepare for the following definition and analysis of the Poincaré map, we first define two straight lines as follows:

$$l_3 : S = S_v \text{ and } l_4 : S = S_u$$

with $S_u \doteq [1 - \eta_1 S_v/S_v + h_1]S_v$. Given that $0 < S_v < K$ and substituting $S = S_v$ into $h(S)$ yields the intersection point of two lines l_2 and l_3, denoted by $Q_{S_v} = (S_v, I_{S_v})$ with

$$I_{S_v} = \frac{\Lambda - \delta S_v}{\beta S_v}$$
$$I_{S_v} = \frac{\Lambda - \delta S_v}{\beta S_v}$$

Similarly, we can get the intersection point of the two lines l_2 and l_4, denoted by $Q^+_{S_u} = (S_u, I_{S_u})$ with $I_{S_u} = \Lambda - \delta S_u/\beta S_u$.

2.2 Existence and Stability of the Disease Free Periodic Solution. Let $I(t) = 0$ and consider the following subsystem:

$$\begin{cases} \dfrac{dS(t)}{dt} = \Lambda - \delta S, \quad S(t) < S_v \\ S(t^+) = \left[1 - \dfrac{\eta_1 S(t)}{S(t) + h_1}\right] S(t), \quad S(t) = S_v \end{cases} \tag{3}$$

Solving Eq. (3) with initial value $S_0 = S(0^+) = S_{u,}$ we can obtain the following periodic solution:

$$S^{\mathrm{T}}(t) = K - (K - S_u)\exp(-\delta t)$$

with period

$$T = \int_{S_u}^{S_v} \frac{1}{\Lambda - \delta S} dS = -\frac{1}{\delta} \ln\left(\frac{K - S_v}{K - S_u}\right)$$

This indicates that a DFPS exists for model (2), denoted by $(S^{\mathrm{T}}(t), 0)$, and for its stability, we have the following main results

THEOREM 1. *If $R_0 \le 1$, then the DFPS $(S^T(t), 0)$ of model (2) is globally asymptotically stable.*

Proof 1. It follows from Lemma A.1 in the Appendix that we have $\phi(S, I) = S - S_v$, $\sigma_1(S, I) = -(\eta_1 S^2/S + h_1)$ and $\sigma_2(S, I) = -(\eta_2 I^2/I + h_2)$. By simple calculation, one has

$$\frac{\partial \sigma_2}{\partial I}\frac{\partial \phi}{\partial S} - \frac{\partial \sigma_2}{\partial S}\frac{\partial \phi}{\partial I} + \frac{\partial \phi}{\partial S} = 1 - \frac{\eta_2 I(I + 2h_2)}{(h_2 + I)^2},$$
$$\frac{\partial \sigma_1}{\partial S}\frac{\partial \phi}{\partial I} - \frac{\partial \sigma_1}{\partial I}\frac{\partial \phi}{\partial S} + \frac{\partial \phi}{\partial I} = 0$$

and $\Delta_1 = (1 - (\eta_2 I(I + 2h_2)/(h_2 + I)^2))P_+/P = (1 - (\eta_2 I(I + 2h_2)/(h_2 + I)^2))K - S_u/K - S_v$. Moreover

$$\int_0^T \left(\frac{\partial P}{\partial S} + \frac{\partial Q}{\partial I}\right) dt = \int_0^T (\beta S^{\mathrm{T}}(t) - \delta - q) dt$$
$$\doteq J_1 + J_2 + J_3$$

where

$$J_1 = -\delta T = \ln\left(\frac{K - S_v}{K - S_u}\right)$$

$$J_2 = \int_0^T \beta S^{\mathrm{T}}(t) dt = \int_{S_u}^{S_v} \frac{\beta S}{\Lambda - \delta S} dS = \frac{\beta}{\delta}\left(K \ln \frac{K - S_u}{K - S_v} + S_u - S_v\right)$$

and

$$J_3 = -qT = \int_{S_u}^{S_v} \frac{-q}{\Lambda - \delta S} dS = \frac{q}{\delta} \ln\left(\frac{K - S_v}{K - S_u}\right)$$

In particular, if $h_2 = 0$, then we have $B_2'(0) = -\eta_2$ with $\Delta_1 = (1 - \eta_2)\frac{K - S_u}{K - S_v}$; if $h_2 \neq 0$, then $B_2'(0) = 0$ with $\Delta_1 = \frac{K - S_u}{K - S_v}$. Therefore, we have $\mu_2 = \exp(J_2 + J_3) > 0$ for $h_2 \neq 0$, and $\mu_2 = (1 - \eta_2)\exp(J_2 + J_3) > 0$ for $h_2 = 0$.

It follows from the monotonicity of the function $\omega_1(x) \doteq \ln(1 - x) + x$ and inequalities $0 < S_u < S_v \le K$ that we have $J_2 > 0$. Obviously, $J_3 < 0$ holds, and we have

$$\begin{aligned} J_2 + J_3 &= \int_{S_u}^{S_v} \frac{\beta S - q}{\Lambda - \delta S} dS \\ &= -\frac{\beta}{\delta}(S_v - S_u) + \frac{1}{\delta}(\beta K - q)\ln\left(\frac{K - S_u}{K - S_v}\right) \\ &= \frac{q}{\delta}\left[(R_0 - 1)\ln\left(\frac{K - S_u}{K - S_v}\right) - \frac{\beta}{q}(S_v - S_u)\right] \\ &= \frac{q}{\delta}\left[(R_0 - 1)\ln\left(\frac{R_0 - \dfrac{S_u}{S^*}}{R_0 - \dfrac{S_v}{S^*}}\right) - \left(\frac{S_v}{S^*} - \frac{S_u}{S^*}\right)\right] \\ &< \frac{q(R_0 - 1)}{\delta} \ln\left(\frac{K - S_u}{K - S_v}\right) \end{aligned} \tag{4}$$

which indicates that if $R_0 \le 1$, then we have $\mu_2 < 1$, and consequently, the DFPS is locally stable.

For the global stability, we only need to show that the DFPS $(S^{\mathrm{T}}(t), 0)$ is globally attractive. To do this, we assume, without loss of generality, that the impulsive point series I_k^+ of any solution starting from the l_4 with $I_k^+ \in [0, I_{S_u}]$ for all $k \ge 0$. It follows from $R_0 \le 1$ and $S_v < K$ that we have $dI/dt < 0$ for $S \le S_v$. Thus, it follows from the properties of the function $f(I)$ that $\{I_k^+\}$ is a strictly decreasing sequence with $\lim_{k \to +\infty} I_k^+ = I_0$, as shown in Fig. 1(*b*). Moreover, we claim that $I_0 = 0$ must hold; otherwise, it contradicts $dI/dt < 0$ for $S \le S_v$. Therefore, the DFPS $(S^{\mathrm{T}}(t), 0)$ is globally attractive. This completes the proof.

Remark 1. It follows from the proof of Theorem 1 that $R_0 \le 1$ implies $\mu_2 < 1$, which means that the nonexistence of the interior equilibrium for uncontrolled system (1) indicates the existence and global stability of the DFPS $(S^{\mathrm{T}}(t), 0)$ of controlled system (2). Naturally, we can define the multiplier μ_2 as the control reproduction number, denoted by R_c with

$$R_c = \exp(J_2 + J_3) > 0 \text{ for } h_2 \neq 0, \text{ and}$$
$$R_c = (1 - \eta_2)\exp(J_2 + J_3) > 0 \text{ for } h_2 = 0$$

and interesting questions that arise are as follows: (a) whether or not the threshold dynamical behavior of model (2) is determined by R_c? (b) how to determine the dynamics of model (2) when $\mu_2 = R_c < 1 < R_0$ or $R_c > 1$?

Remark 2. The relationships between R_0 and R_c have been shown in Figs. 1(*a*) and 1(*c*) for $R_0 < 1$ and $R_0 > 1$, respectively. Although $R_0 \le 1$ indicates $R_c < 1$ (Fig. 1(*a*)), we found that R_c could be larger than R_0 once the threshold S_v is less than the critical value $\bar{S}_v$. This confirms that the implementation of integrated control measures is not conducive to the elimination of the disease when the control threshold level S_v is less than the critical value $\bar{S}_v$. While for $R_0 > 1$, the relations between the R_0 and R_c could be more complex, which will be addressed in Sec. 5. It is interesting to note that the reproduction number R_c is a nonmonotonic function of S_v, and there exists a critical value, denoted by $\hat{S}_v$, such that R_c reaches its minimal value. This clarifies that the correct selection of the threshold level S_v is beneficial to the control of the disease. However, the DFPS and interior equilibrium P^* could coexist and bistability occurs in this case, which reveals some interesting dynamics related to the transcritical and backward bifurcations for model (2) (see more details in the coming sections), as shown in Fig. 1(*d*).

3 Poincaré Map and Dynamics of Model (2) for $R_0 \le 1$

Although the global dynamics of model (2) for $R_0 \le 1$ have been given in Theorem 1, in order to address the threshold dynamics related to R_c and all possible dynamics for $R_0 > 1$, we need to develop new methods, described below.

3.1 The Definition of the Poincaré Map. Denote $V_{S_v} = \{(S,I)|S = S_v, I \ge 0\}$ and $V_{S_u} = \{(S,I)|S = S_u, I \ge 0\}$. We choose the section V_{S_u} as a Poincaré section. Assume that the point $P_k^+ = (S_u, I_k^+)$ lies in the section V_{S_u}, and the trajectory initiating from P_k^+ will reach the section V_{S_v} in a finite time, denote the intersection point as $P_{k+1} = (S_v, I_{k+1})$, where I_{k+1} is determined by I_k^+. Without loss of generality, we can assume that $I_{k+1} \doteq \mathcal{P}(I_k^+)$ is determined by the trajectory of model (1). A single state-dependent feedback control action is implemented at point P_{k+1} such that it jumps to point $P_{k+1}^+ = (S_u, I_{k+1}^+)$ with $I_{k+1}^+ = I_{k+1} + B_2(I_{k+1})$ on V_{S_u}. Therefore, we can define the Poincaré map P_M as

$$I_{k+1}^+ = \mathcal{P}(I_k^+) + B_2(I_{k+1}) \doteq P_M(I_k^+) \tag{5}$$

Now, we define the impulsive set M as

$$\mathcal{M} = \{(S,I) \in R_+^2 | S = S_v, 0 \le I \le I_M\}$$

which is a closed subset of R_+^2, where $I_M = \mathcal{P}(I_{S_u})$ for $R_0 \le 1$. Define the continuous function $F : (S_v, I) \in \mathcal{M} \to (S^+, I^+) = (S_u, f(I)) \in R_+^2$, where $f(I)$ is continuous and increasing in $[0, I_M]$. Thus, the phase set can be defined as follows:

$$\mathcal{N} = F(\mathcal{M}) = \{(S^+, I^+) \in R_+^2 | S^+ = S_u, 0 \le I^+ \le f(I_M)\}$$

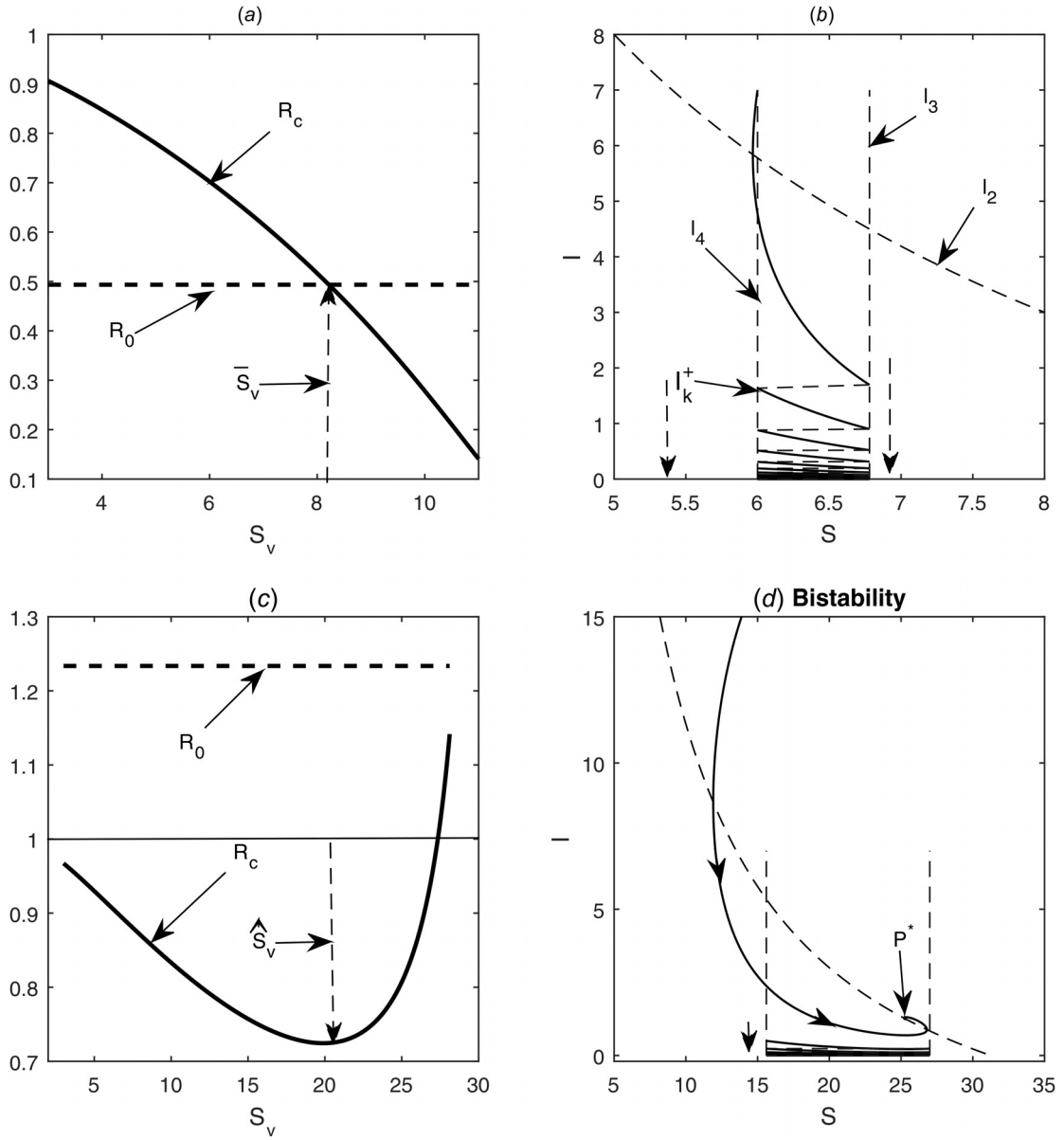

Fig. 1 The relationship between R_0 and R_c in (*a*) and (*c*), and the global stability of the DFPS and bistability in (*b*) and (*d*). The parameter values are as follows: $\Lambda = 1$ in (*a*) and (*b*) with $S_v = 6.78$ and $\eta_1 = 0.2$, $\Lambda = 2.5$ in (*c*) and (*d*) with $S_v = 27$ and $\eta_1 = 0.5$. The other parameter values are as follows: $\beta = 0.015$, $\delta = 0.08$, $\gamma = 0.3$, $h_1 = 5$, $\eta_2 = 0.1$, $h_2 = 3$.

Meanwhile, the Poincaré map P_M can be determined by the impulsive points in the phase set according to the phase portrait. To show this, we define a scalar differential equation in phase space

$$\begin{cases} \dfrac{dI}{dS} = \dfrac{I[-q+\beta S]}{\Lambda - \delta S - \beta SI} \doteq G(S,I) \\ I(S_u) = I_0^+ \end{cases} \tag{6}$$

For model (6), we only focus on the region

$$\Omega = \{(S,I) | S > 0, I > 0, I < h(S)\} \tag{7}$$

in which the function $G(S, I)$ is continuously differentiable. Further, we denote $I_0^+ \doteq Y$ with $Y \in \mathcal{N}$ and $Y < I_{S_u}$, i.e., we have $(S_0^+, Y) \in \Omega$. Then we have

$$I(S) = I(S; S_u, Y) = I(S,Y), S_u \le S \le S_v$$

and

$$I(S,Y) = Y + \int_{S_u}^{S} G(s, I(s,Y))ds$$

Thus, P_M takes the form in Ω

$$\begin{aligned} P_M(I_k^+) &= I_{k+1}^+ = I(S_v, I_k^+) + B_2(I(S_v, I_k^+)) \\ P_M(Y) &= I(S_v, Y) + B_2(I(S_v, Y)) = f(I(S_v, Y)) \end{aligned}$$

THEOREM 2. *For $R_0 \le 1$, the Poincaré map P_M of model (2) satisfies the following properties*:

(a) *the domain and range of P_M are $[0, I_{S_u}] \cup (I_{S_u}, +\infty)$ and $[0, P_M(I_{S_u})]$, respectively. Moreover, P_M is continuous and concave on the interval $[0, I_{S_u}]$.*
(b) *P_M has a unique fixed point $I = 0$, which is globally stable, i.e., the DFPS of model (2) is globally stable.*

Proof 2. By simple calculations, we have

$$\begin{aligned} \frac{\partial G(S,I)}{\partial I} &= \frac{(\Lambda - \delta S)(-q + \beta S)}{(\Lambda - \delta S - \beta SI)^2}, \\ \frac{\partial^2 G(S,I)}{\partial I^2} &= \frac{2(\Lambda - \beta S)\beta S(-q + \beta S)}{(\Lambda - \delta S - \beta SI)^3} \end{aligned}$$

It follows from $S_u \le S_v < K$ and $R_0 \le 1$ that $\Lambda - \delta S > 0$ and $-q + \beta S < 0$ for $S \le S_v$, while $\Lambda - \delta S - \beta SI > 0$ for $I < I_{S_u}$ and $\Lambda - \delta S - \beta SI < 0$ for $I > I_{S_u}$. All these results confirm that $\frac{\partial G(S,I)}{\partial I} < 0$ and $\frac{\partial^2 G(S,I)}{\partial I^2} < 0$ for all $I < I_{S_u}$.

According to the theorem of Cauchy and Lipschitz with parameters on the scalar differential equation, we have

$$\frac{\partial I(S,Y)}{\partial Y} = \exp\left(\int_{S_u}^{S} \frac{\partial}{\partial I} G(s, I(s,Y))ds\right) > 0$$

and

$$\frac{\partial^2 I(S,Y)}{\partial Y^2} = \frac{\partial I(S,Y)}{\partial Y} \int_{S_u}^{S} \frac{\partial^2}{\partial I^2} G(s, I(s,Y)) \frac{\partial I(s,Y)}{\partial Y} ds < 0 \tag{8}$$

Furthermore, it follows from the definition of the function:

$$P_M(Y) = I(S_v, Y)\left(1 - \frac{\eta_2 I(S_v, Y)}{h_2 + I(S_v, Y)}\right) = f(I(S_v, Y))$$

that we have

$$\begin{aligned} \frac{\partial P_M(Y)}{\partial Y} &= \left(1 - \frac{\eta_2 I(S_v,Y)(I(S_v,Y) + 2h_2)}{(h_2 + I(S_v,Y))^2}\right) \frac{\partial I(S_v,Y)}{\partial Y} \\ &= \left(1 - \frac{\eta_2 I(S_v,Y)(I(S_v,Y) + 2h_2)}{(h_2 + I(S_v,Y))^2}\right) \\ &\quad \times \exp\left(\int_{S_u}^{S_v} \frac{\partial}{\partial I} G(s, I(s,Y))ds\right) \\ &= f'(I(S_v,Y)) \exp\left(\int_{S_u}^{S_v} \frac{\partial}{\partial I} G(s, I(s,Y))ds\right) \end{aligned} \tag{9}$$

and

$$\begin{aligned} \frac{\partial^2 P_M(Y)}{\partial Y^2} &= \frac{\partial^2 I(S_v,Y)}{\partial Y^2} + \frac{\partial^2 I(S_v,Y)}{\partial Y^2} \frac{\partial B_2(I)}{\partial I}\bigg|_{I=I(S_v,Y)} \\ &\quad + \frac{\partial I(S_v,Y)}{\partial Y}\left(\frac{\partial}{\partial Y}\frac{\partial B_2(I)}{\partial I}\bigg|_{I=I(S_v,Y)}\right) \\ &= \left(B_2'(I(S_v,Y)) + 1\right)\frac{\partial^2 I(S_v,Y)}{\partial Y^2} + \left(\frac{\partial I(S_v,Y)}{\partial Y}\right)^2 B_2''(I(S_v,Y)) \\ &= f'(I(S_v,Y))\frac{\partial^2 I(S_v,Y)}{\partial Y^2} - \left(\frac{\partial I(S_v,Y)}{\partial Y}\right)^2 \frac{2\eta_2 h_2^2}{(I(S_v,Y) + h_2)^3} \end{aligned} \tag{10}$$

Note that if $h_2 = 0$, then $B_2''(0) = 0$; thus, one term $-(2\eta_2/h_2)$ will disappear from the formula for $\partial^2 P_M(0)/\partial Y^2$. Then, it follows from the monotonicity of the function $f(I)$ that if $Y \in (0, I_{S_u}]$, then $(\partial P_M(Y)/\partial Y) > 0$ and $(\partial^2 P_M(Y)/\partial Y^2) < 0$, which indicate that $P_M(Y)$ is continuous and concave on the interval $(0, I_{S_u}]$. Further, according to the monotonicity of $P_M(Y)$ on the interval $(0, I_{S_u}]$, we see that $P_M(Y)$ is monotonically decreasing on the interval $(I_{S_u}, +\infty)$. Therefore, it follows from $R_0 \ge 1$ and $S_v < K$ that $dI/dt \le 0$ for all $S < S_v$, which indicates that $Y \ge \mathcal{P}(Y) > P_M(Y)$ for all $Y \in (0, I_{S_u}] \cup (I_{S_u}, K)$ due to $f(I) < I$. All these results confirm that the Poincaré map P_M only has zero fixed point, i.e., $P_M(0) = 0$, which is globally stable. Consequently, for model (2), there exists a unique DFPS, which is globally stable.

Remark 3. It follows from the proofs of Theorems 1 and 2 that the global stability of the DFPS can be proved by using different methods, and the methods shown in Theorem 2 could be widely employed in generalized systems.

4 Bifurcation and Reproduction Number

Note that if $R_0 > 1$, then for model (1), there exists a unique endemic equilibrium $P^*(S^*, I^*)$. Thus, according to the positions among S_v, $S,^*$ and K, we consider the following two cases

$$(C1),\ \ S_v \le S^* < K, \text{ i.e. } \ R_0 > 1 \ge \frac{\beta S_v}{q}$$

$$(C2),\ \ S^* < S_v < K, \text{ i.e. } 1 < \frac{\beta S_v}{q} < R_0$$

For case $(C1)$, any solution initiating from the line l_4 will experience infinitely many impulsive effects. Moreover, it follows from $(\beta S - q/\Lambda - \delta S) < 0$ for all $S \in [S_u, S_v]$ due to $S_v \le S^*$ that we have $J_2 + J_3 < 0$, i.e., $R_c < 1$. This indicates that the DFPS is locally stable for case $(C1)$.

Moreover, for case $(C1)$, the Poincaré map P_M is well defined, which satisfies all properties shown in Theorem 2 by using similar methods. Thus, for case $(C1)$, we have the following main results:

THEOREM 3. *If $R_0 > 1 \ge \beta S_v/q$ then the DFPS $(S^T(t), 0)$ of model (2) is globally stable*.

Remark 4. Under the conditions of Theorem 3, we see that the uncontrolled ordinary differential equation model will be stable in the endemic state $P^*(S^*, I^*)$, as shown in Fig. 2(*d*). If so, we only need to correctly choose the threshold of the susceptible population S_v, i.e., $S_v < S^*$, then the disease can be successfully controlled such that it quickly declines toward extinction, as shown in Figs. 2(*a*)–2(*c*).

For case (*C*2), since the sign of $J_2 + J_3$ can vary, the DFPS could be unstable in this case. Thus, interesting dynamics may occur as parameter values vary. For convenience, we only need to assume that the Poincaré map P_M is well defined in the domain $U(0^+) = [0, \epsilon)$ for $\epsilon > 0$ small enough in the following, as shown in Fig. 1(*d*), from which we can see that the P_M is only well defined in a small interval $U(0^+) = [0, \epsilon)$. Based on this assumption, we address the bifurcations related to the DFPS and discuss the threshold dynamics determined by the R_0 and R_c in the following.

4.1 Transcritical and Pitchfork Bifurcations for η_1. In this subsection, we choose η_1 as the bifurcation parameter and focus on $h_2 \neq 0$ first. Thus, we consider $J_2 + J_3$ as a function of η_1, i.e.,

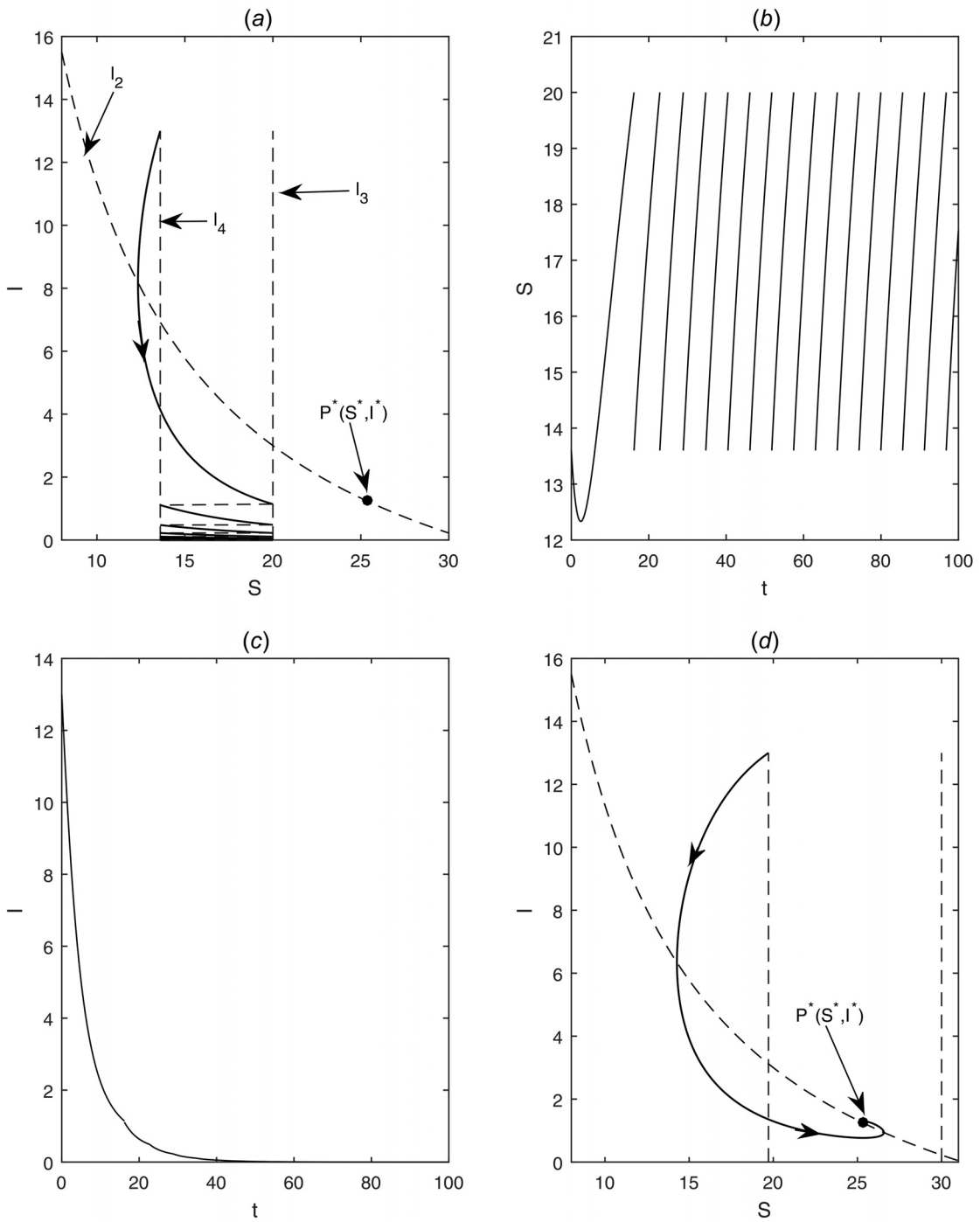

Fig. 2 Illustration of the global stability of the DFPS for case (*C*1), i.e., $R_0 > 1 \geq \beta S_v/q$. The parameter values are as follows: $\Lambda = 2.5$, $\beta = 0.015$, $\delta = 0.08$, $\gamma = 0.3$, $\eta_1 = 0.4$, $h_1 = 5$, $\eta_2 = 0.1$, $h_2 = 3$, and $S_v = 20$ in (*a*)–(*c*), $S_v = 30$ in (*d*).

$$J_{12}(\eta_1) \doteq J_2 + J_3 = -\frac{\beta}{\delta}(S_v - S_u) + \frac{1}{\delta}(\beta K - q)\ln\left(\frac{K - S_u}{K - S_v}\right),\ R_c(\eta_1) = \exp\left(J_{12}(\eta_1)\right)$$

with $S_u = S_v + B_1(S_v, \eta_1)$. By simple calculation, we have

$$\frac{\partial S_u}{\partial \eta_1} = \frac{\partial B_1(S_v, \eta_1)}{\partial \eta_1} = -\frac{S_v^2}{S_v + h_1} < 0$$

and

$$\frac{dR_c(\eta_1)}{d\eta_1} = \exp\left(J_{12}(\eta_1)\right)\frac{\partial B_1(S_v, \eta_1)}{\partial \eta_1}\left(-\frac{\beta S_u - q}{\Lambda - \delta S_u}\right)$$

Solving $dR_c(\eta_1)/d\eta_1 = 0$ with respect to η_1 yields a unique root, denoted by $\bar{\eta}_1$, which is equivalent to the unique root of the equation $S_u = S^*$, i.e.,

$$\bar{\eta}_1 = \left(1 - \frac{S^*}{S_v}\right)\left(1 + \frac{h_1}{S_v}\right) > 0$$

In order to ensure that $\bar{\eta}_1$ (i.e., $0 < \bar{\eta}_1 \le 1$), we need $(S_v h_1/S_v + h_1) \le S^* < S_v$.

Note that if $\eta_1 \in (0, \bar{\eta}_1)$, then we have $S_u > S^*$ and $dR_c(\eta_1)/d\eta_1 > 0$; if $\eta_1 \in (\bar{\eta}_1, 1)$, then we have $S_u < S^*$ and $dR_c(\eta_1)/d\eta_1 < 0$. Moreover, it follows from $R_c(0) = 1$ and $R_c(\bar{\eta}_1) = \exp(\int_{S^*}^{S_v} \frac{\beta s - q}{\Lambda - \delta s} ds) > 1$ that $R_c(\eta_1) > 1$ for $S_u > S^*$ (i.e., $\eta_1 \in (0, \bar{\eta}_1)$). Thus, the DFPS is unstable and bifurcation does not occur at all. If $S_u < S^*$ (i.e., $\eta_1 \in (\bar{\eta}_1, 1)$), then the bifurcation could occur, provided that there exist $\eta_1^* \in (\bar{\eta}_1, 1)$ with $R_c(\eta_1^*) = 1$, which means that we need $R_c(1) < 1$. Further, according to the monotonicity of $R_c(\eta_1)$, we conclude that η_1^* is unique. All these results confirm that if $0 < \eta_1 < \eta_1^*$, then the periodic solution $(S^T(t), 0)$ is unstable; if $1 > \eta_1 > \eta_1^*$, then the periodic solution $(S^T(t), 0)$ is stable. This shows that the possible bifurcation could occur at $\eta_1 = \eta_1^*$.

Furthermore, if $\eta_1 = 1$, then $S_u = h_1 S_v/h_1 + S_v$. It follows from $(K - S_u/K - S_v) > 1$ that

$$\ln\left(\frac{K - S_u}{K - S_v}\right) < \frac{\frac{K - S_u}{K - S_v} - 1}{\sqrt{\frac{K - S_u}{K - S_v}}} = \frac{S_v - S_u}{\sqrt{(K - S_u)(K - S_v)}}$$

Therefore, we have

$$J_{12}(1) = \frac{\beta}{\delta}\left[-(S_v - S_u) + (K - S^*)\ln\left(\frac{K - S_u}{K - S_v}\right)\right] < \frac{\beta}{\delta}(S_v - S_u)\left[-1 + \frac{(K - S^*)}{\sqrt{(K - S_u)(K - S_v)}}\right]$$

That is, in order to ensure that $J_{12}(1) < 0$ (i.e., $R_c(1) < 1$), we only need $K - S^* < \sqrt{(K - S_v)(K - S_u)}$, i.e., $\frac{h_1 S_v}{h_1 + S_v} < K - \frac{(K - S^*)^2}{K - S_v}$ with $K - \frac{(K - S^*)^2}{K - S_v} < S^*$. According to

$$0 < \frac{h_1 S_v}{h_1 + S_v} < K - \frac{(K - S^*)^2}{K - S_v} = S^*\left[R_0 - \frac{(R_0 - 1)^2}{R_0 - \frac{S_v}{S^*}}\right]$$

we have $S^* > K - \sqrt{K(K - S_v)}$ (i.e., $R_0 > \frac{1}{2 - \frac{S_v}{S^*}} > 1$). Based on the above discussion, we have the following main results related to the bifurcation parameter η_1 and reproduction number R_c.

THEOREM 4. *If* $1 < \frac{S_v}{S^*} < R_0$, $R_c(1) < 1$ *and* $M \doteq \frac{\partial^2 I(S_v, 0)}{\partial Y^2} < \frac{2\eta_2}{h_2}$, *then* $P_M(Y, \eta_1)$ *and the transcritical bifurcation occurs at* $\eta_1 = \eta_1^*$. *That is, a stable positive fixed point of the* $P_M(Y, \eta_1)$ *appears when the parameter* η_1 *changes through* η_1^* *from right to left. Correspondingly, system (2) has a stable positive periodic solution if* $\eta_1 \in (\eta_1^* - \epsilon, \eta_1^*)$ *with* $\epsilon > 0$ *small enough. However, if* $M > 2\eta_2/h_2$, *an unstable positive fixed point of the* $P_M(Y, \eta_1)$ *appears when the parameter* η_1 *changes through* η_1^* *from left to right. Correspondingly, system (2) has an unstable positive periodic solution if* $\eta_1 \in (\eta_1^*, \eta_1^* + \epsilon)$ *with* $\epsilon > 0$ *small enough.*

Proof 3. Since $P_M(Y, \eta_1)$ is well defined in the domain $U(0^+) = [0, \epsilon)$, we see that it is continuous and differentiable. In order to prove Theorem 4, we only need to verify that P_M satisfies the four conditions of Lemma A.2 in the Appendix.

Letting $I(S; S_u, Y) = I(S, Y)$, we have $P_M(Y, \eta_1) = I(S_v, Y)$ and $P_M(0, \eta_1) = I(S_v, 0) = 0$, which indicates that the first condition of Lemma A.2 holds true. According to the inequality (9), we have

$$\frac{\partial P_M(0, \eta_1)}{\partial Y} = \exp\left(\int_{S_u}^{S_v} \frac{\beta S - q}{\Lambda - \delta S} dS\right) = R_c(\eta_1)$$

Thus, $\frac{\partial P_M(0, \eta_1^*)}{\partial Y} = R_c(\eta_1^*) = 1$ and the second condition of Lemma A.2 follows.

By simple calculations, we have

$$\frac{\partial^2 P_M(0, \eta_1)}{\partial Y \partial \eta_1} = \frac{\partial S_u}{\partial \eta_1}\frac{\partial}{\partial S_u}\left(\frac{\partial P_M(0, \eta_1)}{\partial Y}\right) = \frac{\partial S_u}{\partial \eta_1}\frac{\partial}{\partial S_u}\left(\frac{\partial I(S_v, Y)}{\partial Y}\right) = \left(\frac{\partial I(S_v, Y)}{\partial Y}\right)\frac{\partial S_u}{\partial \eta_1}\frac{\partial}{\partial S_u}\int_{S_u}^{S_v}\frac{\partial G(s, I(s, 0))}{\partial Y} ds = \frac{dR_c(\eta_1)}{d\eta_1} \tag{11}$$

which indicates that $\frac{\partial^2 P_M(0, \eta_1)}{\partial Y \partial \eta_1} = \frac{dR_c(\eta_1^*)}{d\eta_1} < 0$, and the third condition of Lemma A.2 follows.

Further, it follows from inequality (10) that:

$$\frac{\partial^2 P_M(0, \eta_1)}{\partial Y^2} = \exp(J_{12})\int_{S_u}^{S_v}\frac{\partial^2}{\partial I^2}(G(s, I(s, 0)))\frac{\partial I(s, 0)}{\partial Y} ds - \frac{2\eta_2}{h_2}\exp(2J_{12}) \tag{12}$$

Denote

$$l_1(s) = \int_{S_u}^{s}\frac{\beta s - q}{\Lambda - \delta s} ds$$

$$k_1(s) = \frac{\partial I(s, 0)}{\partial Y} = \exp\left(\int_{S_u}^{s}\frac{\beta s - q}{\Lambda - \delta s} ds\right) = \exp l_1(s)$$

and it is easy to know that $k_1(S_u) = 1$ and $k_1(S_v) = R_c(\eta_1)$. Taking the derivative of $l_1(s)$ with respect to s yields

$$l_1'(s) = \frac{\beta s - q}{\Lambda - \delta s}$$

Letting

$$l_2(s) = \frac{\partial^2}{\partial I^2}G(s, I(s, 0)) = \frac{2\beta s(-q + \beta s)}{(\Lambda - \delta s)^2},\ k_2(s) = \frac{l_2(s)}{l_1'(s)} = \frac{2\beta s}{\Lambda - \delta s} = \frac{2}{h(s)}$$

and $S_{u\eta_1^*} = (1 - \frac{\eta_1^* S_v}{S_v + h_1})S_v$, then we have

$$\frac{\partial^2 P_M(0, \eta_1^*)}{\partial Y^2} = \frac{\partial^2 I(S_v, 0)}{\partial Y^2} - \frac{2\eta_2}{h_2} \tag{13}$$

where

$$M \doteq \frac{\partial^2 I(S_v,0)}{\partial Y^2} = \int_{S_{u\eta_1^*}}^{S_v} \frac{\partial^2}{\partial I^2}(G(s,I(s,0)))\frac{\partial I(s,0)}{\partial Y}ds$$
$$= \int_{S_{u\eta_1^*}}^{S_v} l_2(s)k_1(s)ds$$
$$= \int_{S_{u\eta_1^*}}^{S_v} \frac{l_2(s)}{l_1'(s)} l_1'(s)\exp l_1(s)ds \quad (14)$$
$$= \int_{S_{u\eta_1^*}}^{S_v} k_2(s)d(k_1(s))$$

Note that the function $k_1(s)$ is monotonically decreasing on the interval $[S_u, S^*]$ and monotonically increasing on the interval $[S^*, S_v]$, which indicates that if $\eta_1 = \eta_1^*$ then $k_1(S_{u\eta_1^*}) = R_c(\eta_1^*) = 1$. Thus, $k_1(S^*) < k_1(s) \le 1$ for all $s \in [S_{u\eta_1^*}, S_v]$. According to $k_2'(s) = \frac{2\Lambda\beta}{(\Lambda-\beta s)^2} > 0$ for any $s \in [S_{u\eta_1^*}, S_v]$, $k_2(s)$ is a monotonically increasing function. Moreover, we have

$$\int_{S_{u\eta_1^*}}^{S_v} k_2(s)d(k_1(s)) = k_1(s)k_2(s)|_{S_{u\eta_1^*}}^{S_v} - \int_{S_{u\eta_1^*}}^{S_v} k_1(s)k_2'(s)ds$$
$$= k_2(S_v) - k_2(S_{u\eta_1^*}) - \int_{S_{u\eta_1^*}}^{S_v} k_1(s)k_2'(s)ds \quad (15)$$
$$= \int_{S_{u\eta_1^*}}^{S_v} (1-k_1(s))k_2'(s)ds$$

which means that

$$0 < M < (1-k_1(S^*))(k_2(S_v) - k_2(S_{u\eta^*})).$$

Therefore, if $1 \le \frac{S_v}{S^*} < R_0$, $R_c(1) < 1$ and $M \ne \frac{2\eta_2}{h_2}$, then the transcritical bifurcation occurs at $\eta_1 = \eta_1^*$. Furthermore, if $M > \frac{2\eta_2}{h_2}$, then $P_M(Y, \eta_1)$ generates an unstable fixed point when η_1 passes η_1^* from left to right. That is, for $\eta_1 \in (\eta_1^*, \eta_1^* + \epsilon)$ with $\epsilon > 0$ small enough, an unstable positive periodic solution exists for model (2), as shown in Fig. 1(*d*). While, if $M < \frac{2\eta_2}{h_2}$, then $P_M(Y, \eta_1)$ exists with a positive stable fixed point when η_1 goes through η_1^* from right to left. That is, for $\eta_1 \in (\eta_1^* - \epsilon, \eta_1^*)$ with $\epsilon > 0$ small enough, a stable positive periodic solution exists for model (2).

Corollary 1. *If* $1 < \frac{\beta S_v}{q} < R_0$, $R_c(1) < 1$ *and* $M > \frac{2\eta_2}{h_2}$, *system (2) undergoes the backward bifurcation at* $\eta_1 \in (\eta_1^*, \eta_1^* + \epsilon)$ *with* $\epsilon > 0$ *small enough.*

Note that the condition $R_c(1) < 1$ can be replaced by the inequality $\frac{h_1 S_v}{h_1 + S_v} < K - \frac{(K-S^*)^2}{K-S_v}$. It follows from the conditions of Corollary 1 that the positive equilibrium P^* exists, which is stable for model (2) due to $S_v > S^*$. Moreover, the DFPS $(S^T(t), 0)$ is stable for all $\eta_1 \in (\eta_1^*, 1)$, i.e., we have $R_c(\eta_1) < 1$ for all $\eta_1 \in (\eta_1^*, 1)$. Therefore, the stable DFPS $(S^T(t), 0)$ and stable equilibrium P^* can coexist, as shown in Fig. 1(*d*), and there exists an unstable order-1 periodic solution, which is bifurcated from $(S^T(t), 0)$ once the parameter η_1 increases and exceeds the critical value η_1^*. Obviously, the transcritical bifurcation generates a backward bifurcation, which is a novel result generated by the state-dependent pulse vaccination model (2).

In the following, we address the special case, i.e., $M = 2\eta_2/h_2$. For this special case, we only need to calculate $\frac{\partial^3 P_M(0,\eta_1^*)}{\partial Y^3}$, i.e.,

$$\frac{\partial^3 P_M(0,\eta_1^*)}{\partial Y^3} = \frac{\partial^3 I(S_v,0)}{\partial Y^3} + 3\int_{S_{u\eta_1^*}}^{S_v} k_2(s)d(\exp l_1(s))B_2''(0) + B_2'''(0)$$
$$= \frac{\partial^3 I(S_v,0)}{\partial Y^3} - \frac{6\eta_2}{h_2}M + \frac{6\eta_2}{h_2^2}$$
$$= \frac{\partial^3 I(S_v,0)}{\partial Y^3} - \frac{12\eta_2^2}{h_2^2} + \frac{6\eta_2}{h_2^2} \quad (16)$$

where

$$\frac{\partial^3 I(S_v,0)}{\partial Y^3} = \frac{4\eta_2^2}{h_2^2} + \frac{\partial}{\partial Y}\left(\int_{S_{u\eta_1^*}}^{S_v} \frac{\partial^2}{\partial I^2}(G(s,I(s,0)))\frac{\partial I(s,0)}{\partial Y}ds\right) \quad (17)$$

and

$$\frac{\partial}{\partial Y}\left(\int_{S_{u\eta_1^*}}^{S_v} \frac{\partial^2}{\partial I^2}(G(s,I(s,0)))\frac{\partial I(s,0)}{\partial Y}ds\right)$$
$$= \int_{S_{u\eta_1^*}}^{S_v} l_2(s)k_1(s)\left[\frac{3}{2}k_1(s)k_2(s) + l_1(s)\right]ds \quad (18)$$

Therefore, according to Lemma A.3, we have the following main results for this special case:

THEOREM 5. *If* $1 < \frac{S_v}{S^*} < R_0$, $R_c(1) < 1$, $M = \frac{2\eta_2}{h_2}$ *and* $\frac{\partial^3 P_M(0,\eta_1^*)}{\partial Y^3} \ne 0$, *then the Poincaré map of system (2) occurs with a pitchfork bifurcation at* η_1^*. *Furthermore, if* $\frac{\partial^3 P_M(0,\eta_1^*)}{\partial Y^3} < 0$, *then the Poincaré map (2) occurs with a subcritical pitchfork bifurcation such that it appears as a stable positive fixed point; if* $\frac{\partial^3 P_M(0,\eta_1^*)}{\partial Y^3} > 0$, *then the Poincaré map (2) occurs with a supercritical pitchfork bifurcation such that it appears as an unstable positive fixed point.*

Note that the formula of R_c depends on the h_2, in particular if $h_2 = 0$, then we have $R_c(\eta_1) = (1-\eta_2)\exp(J_{12}(\eta_1))$, thus $R_c(0) = 1 - \eta_2$, $R_c(\bar{\eta}_1) > 1 - \eta_2$. It follows from the monotonicity of $J_{12}(\eta_1)$ that $R_c(\eta_1)$ is monotonically increasing on the interval $[0, \bar{\eta}_1]$ and monotonically decreasing on the interval $(\bar{\eta}_1, 1)$. In order to ensure that η_1^* exists and satisfies $R_c(\eta_1^*) = 1$, we need $R_c(\bar{\eta}_1) > 1$, which indicates that $\eta_1^* \in (0, \bar{\eta}_1)$. Further, if we have $R_c(1) < 1$, then there exists a unique $\eta_1^{**} \in (\bar{\eta}_1, 1)$ such that $R_c(\eta_1^{**}) = 1$. Therefore, if both the η_1^* and η_1^{**} exist, then we have

$$\frac{\partial^2 P_M(0,\eta_1^*)}{\partial Y \partial \eta_1} = \frac{dR_c(\eta_1^*)}{d\eta_1} > 0, \quad \frac{\partial^2 P_M(0,\eta_1^{**})}{\partial Y \partial \eta_1} = \frac{dR_c(\eta_1^{**})}{d\eta_1} < 0,$$
$$\frac{\partial^2 P_M(0,\eta_1^*)}{\partial Y^2} = M > 0, \quad \frac{\partial^2 P_M(0,\eta_1^{**})}{\partial Y^2} = M > 0,$$

and consequently we have the following main result:

Corollary 2. *If* $h_2 = 0$, $1 < \frac{S_v}{S^*} < R_0$, $R_c(\bar{\eta}_1) > 1$ *and* $R_c(1) < 1$, *then* $P_M(Y, \eta_1)$ *occurs with the transcritical bifurcation at* $\eta_1 = \eta_1^*$ *and* $\eta_1 = \eta_1^{**}$. *That is, an unstable positive fixed point of the* $P_M(Y, \eta_1)$ *appears when the parameter* η_1 *changes through* η_1^* *from right to left or through* η_1^{**} *from left to right. Correspondingly, system (2) has an unstable positive periodic solution if* $\eta_1 \in (\eta_1^* - \epsilon, \eta_1^*)$ *or* $\eta_1 \in (\eta_1^{**}, \eta_1^{**} + \epsilon)$ *with* $\epsilon > 0$ *small enough.*

Note that when $h_2 = 0$, we could choose η_2 as a bifurcation parameter. If so, we have

$$R_c(\eta_2) = (1-\eta_2)\exp(J_1 + J_2).$$

Letting $R_c(\eta_2) = 1$ and solving it, one has $\eta_2^* = 1 - \exp(-J_1 - J_2)$ such that $R_c(\eta_2^*) = 1$, which requires $J_1 + J_2 > 0$ to ensure that η_2^* is well defined. Moreover, $S_u > S^*$ implies $J_1 + J_2 > 0$ holds true.

It follows from (4) that:

$$J_2+J_3=\frac{q}{\delta}\left[(R_0-1)\ln\left(\frac{R_0-\frac{S_u}{S^*}}{R_0-\frac{S_v}{S^*}}\right)-\left(\frac{S_v}{S^*}-\frac{S_u}{S^*}\right)\right]$$

Denote the function $\omega_4(x)\doteq(R_0-1)\ln(R_0-x)+x$ with $\omega_4'(x)=1-x/R_0-x$. Thus, $\omega_4(x)$ is monotonically increasing on the interval [0, 1), and decreasing on the interval $[1, R_0)$. Moreover, $x=R_0$ is an asymptote of the function $\omega_4(x)$, and both S_u/S^* and $S_v/S^*\in[0,R_0)$, then we have

$$J_2+J_3=\frac{q}{\delta}\left[\omega_4\left(\frac{S_u}{S^*}\right)-\omega_4\left(\frac{S_v}{S^*}\right)\right]$$

It follows from the monotonicity of the function $\omega_4(x)$ that if $S_u>S^*$ then $J_2+J_3>0$. Moreover, $\omega_4(\frac{S_v}{S^*})<\omega_4(0)=(R_0-1)\ln(R_0)$ also indicates that $J_2+J_3>0$. Solving the inequality $\omega_4(\frac{S_v}{S^*})<(R_0-1)\ln(R_0)$, one has $\frac{S_v}{S^*}\geq(R_0-1)\text{LambertW}(-\frac{R_0}{R_0-1}\exp(-\frac{R_0}{R_0-1}))+R_0\doteq\zeta$, and it is easy to see that $\zeta\in(1,R_0)$, where the definition and properties of the Lambert W function can be found in Refs. [27,29,31]. Therefore

$$\frac{\partial P_M(0,\eta_2)}{\partial Y}=R_c(\eta_2),\frac{\partial^2 P_M(0,\eta_2)}{\partial Y\partial\eta_2}=\frac{dR_c(\eta_2)}{d\eta_2}=-\exp(J_1+J_2)<0$$

and

$$\frac{\partial^2 P_M(0,\eta_2^*)}{\partial Y^2}=M>0$$

By methods similar to those above, we can evaluate the conditions of Lemma A.2, to give the following main results:

COROLLARY 3. *If $h_2=0$, $1<\frac{\beta S_v}{q}<R_0$ and $J_2+J_3>0$, then $P_M(Y,\eta_2)$ occurs with the transcritical bifurcation at $\eta_2=\eta_2^*$. That is, an unstable positive fixed point of the $P_M(Y,\eta_2)$ appears when the parameter η_2 changes through η_2^* from left to right. Correspondingly, system (2) has an unstable positive periodic solution if $\eta_2\in(\eta_2^*,\eta_2^*+\epsilon)$ with $\epsilon>0$ small enough. Particularly, the condition of $J_2+J_3>0$ can be strengthened to be $1\leq S_u/S^*$ or $S_v/S^*\geq(R_0-1)\text{LambertW}(-\frac{R_0}{R_0-1}\exp(-\frac{R_0}{R_0-1}))+R_0$.*

4.2 Transcritical Bifurcation for Threshold Level S_v. In this subsection, we choose the threshold level S_v as a bifurcation parameter, which can help us to evaluate how to determine the number in the population to be vaccinated such that the disease could be eradicated. To do this, we consider the control reproduction number R_c as a function of S_v, i.e., we have $R_c(S_v)=\exp(J_{12}(S_v))$ and

$$\begin{aligned}J_{12}(S_v)\doteq J_2+J_3&=\int_{S_u}^{S_v}\frac{\beta s-q}{\Lambda-\delta s}ds\\&=-\frac{\beta}{\delta}(S_v-S_u)+\frac{1}{\delta}(\beta K-q)\ln\left(\frac{K-S_u}{K-S_v}\right)\end{aligned}$$

By simple calculations, we have

$$\frac{dR_c(S_v)}{dS_v}=\exp(J_{12}(S_v))\frac{dJ_{12}(S_v)}{dS_v}$$

and

$$\frac{dJ_{12}(S_v)}{dS_v}=\frac{\partial}{\partial S_v}\int_{S_u}^{S_v}\frac{\beta s-q}{\Lambda-\delta s}ds$$

where $S_u=S_v+B_1(S_v)$. Letting $\omega_3(x)\doteq\frac{\beta x-q}{\Lambda-\delta x}=\frac{\beta(x-S^*)}{\delta(K-x)}$, one has

$$\frac{dJ_{12}(S_v)}{dS_v}=\omega_3(S_v)-\left(1+B_1'(S_v)\right)\omega_3(S_u)\tag{19}$$

If $S_u\leq S^*$, then $\omega_3(S_u)\leq 0$. It follows from $1+B_1'(S_v)>0$ that $\frac{dJ_{12}(S_v)}{dS_v}>0$; If $S_u>S^*$, then $\omega_3(S_u)>0$. Taking the derivative of $\omega_3(x)$ with respect to x yields

$$\omega_3'(x)=\frac{q}{\delta}\frac{R_0-1}{(K-x)^2}>0$$

Thus, we have

$$\begin{aligned}\omega_3(S_v)-(1+B_1'(S_v))\omega_3(S_u)&>\omega_3(S_u)-(1+B_1'(S_v))\omega_3(S_u)\\&=(-B_1'(S_v))\omega_3(S_u)>0\end{aligned}\tag{20}$$

In conclusion, no matter what the position between S_u and S^* is, we always have $\frac{dJ_{12}(S_v)}{dS_v}>0$, i.e., $J_{12}(S_v)$ is a monotonically increasing function of S_v. Moreover, we have

$$\lim_{S_v\to S^*}J_{12}(S_v)=\lim_{S_v\to S^*}\int_{S_u}^{S_v}\omega_3(x)dx=\int_{S^*+B_1(S^*)}^{S^*}\omega_3(x)dx<0$$

and

$$\lim_{S_v\to K}J_{12}(S_v)=\lim_{S_v\to K}\frac{q}{\delta}\left[(R_0-1)\ln\left(\frac{K-S_u}{K-S_v}\right)-\frac{\beta}{q}(S_v-S_u)\right]=+\infty$$

It follows from the continuity of the function $J_{12}(S_v)$ that there exists a unique $S_v^*\in(S^*,K)$ such that $J_{12}(S_v^*)=0$, i.e., there is a unique $S_v^*\in(S^*,K)$ such that $R_c(S_v^*)=1$. Further, by simple calculations we have

$$\frac{\partial P_M(0,S_v)}{\partial Y}=R_c(S_v)$$

and

$$\frac{\partial^2 P_M(0,S_v)}{\partial Y\partial S_v}=\frac{dR_c(S_v)}{dS_v}>0$$

By employing similar methods to those shown in Theorem 4, we can address the signs of $\frac{\partial^2 P_M(0,S_v^*)}{\partial^2 Y}$ and $\frac{\partial^3 P_M(0,S_v^*)}{\partial^3 Y}$. Therefore, we have the following main results:

THEOREM 6. *If $1<S_v/S^*<R_0$ and $M<2\eta_2/h_2$, then $P_M(Y,S_v)$ occurs with the transcritical bifurcation at $S_v=S_v^*$. That is, a stable positive fixed point of the $P_M(Y,S_v)$ appears when the parameter S_v changes through S_v^* from left to right. Correspondingly, system (2) has a stable positive periodic solution if $S_v\in(S_v^*,S_v^*+\epsilon)$ with $\epsilon>0$ small enough. Moreover, if $M>2\eta_2/h_2$, an unstable positive fixed point of the $P_M(Y,S_v)$ appears when the parameter S_v changes through S_v^* from right to left. Correspondingly, system (2) has an unstable positive periodic solution if $S_v\in(S_v^*-\epsilon,S_v^*)$ with $\epsilon>0$ small enough.*

THEOREM 7. *If $1<S_v/S^*<R_0$, $M=2\eta_2/h_2$ and $\frac{\partial^3 P_M(0,S_v^*)}{\partial Y^3}\neq 0$, then the Poincaré map of system (2) occurs with a pitchfork bifurcation at S_v^*. Furthermore, if $\frac{\partial^3 P_M(0,S_v^*)}{\partial Y^3}<0$, then the Poincaré map (2) occurs with a supercritical pitchfork bifurcation such that it appears as a stable positive fixed point; if $\frac{\partial^3 P_M(0,S_v^*)}{\partial Y^3}>0$, then the Poincaré map (2) occurs with a subcritical pitchfork bifurcation such that it appears as an unstable positive fixed point.*

Similarly, for the special case $h_2=0$, we have

$$R_c(S_v)=(1-\eta_2)\exp(J_{12}(S_v))$$

and according to the properties of the function $J_{12}(S_v)$ we have $\frac{\partial^2 P_M(0,S_v)}{\partial Y \partial S_v} = \frac{dR_c(S_v)}{dS_v} > 0$, which indicates that there exists a unique S_v^* such that $J_{12}(S_v^*) = \ln(\frac{1}{1-\eta_2}) > 0$, i.e., $R_c(S_v^*) = 1$. It follows from $\frac{\partial^2 P_M(0,S_v^*)}{\partial Y^2} = M > 0$ and Lemma A.2 that

Corollary 4. *If $h_2 = 0$, $1 < \frac{\beta S_v}{q} < R_0$, then $P_M(Y, S_v)$ occurs with the transcritical bifurcation at $S_v = S_v^*$, i.e., an unstable positive fixed point of the $P_M(Y, S_v)$ appears when the parameter S_v changes through S_v^* from right to left. Correspondingly, system (2) has an unstable positive periodic solution if $S_v \in (S_v^* - \epsilon, S_v^*)$ with $\epsilon > 0$ small enough.*

4.3 Trans-Critical Bifurcation for Λ. In this subsection, we choose Λ as a bifurcation parameter, i.e., we denote $R_c(\Lambda) = \exp(J_{12}(\Lambda)) = P_M(0, \Lambda)$ and

$$J_{12}(\Lambda) \doteq J_2 + J_3 = \int_{S_u}^{S_v} \frac{\beta s - q}{\Lambda - \delta s} ds = -\frac{\beta}{\delta}(S_v - S_u) + \frac{1}{\delta}\left(-q + \beta\left(\frac{\Lambda}{\delta}\right)\right)\ln\left(\frac{-\delta S_u + \Lambda}{-\delta S_v + \Lambda}\right)$$

with

$$\lim_{\frac{\Lambda}{\delta} \to +\infty} J_{12}(\Lambda) = 0, \ \lim_{\frac{\Lambda}{\delta} \to S_v} J_{12}(\Lambda) = +\infty$$

By calculations, we have

$$\frac{dR_c(\Lambda)}{d\Lambda} = \frac{\partial P_M(0,\Lambda)}{\partial Y} = R_c(\Lambda)\frac{dJ_{12}(\Lambda)}{d\Lambda},$$

$$\frac{dJ_{12}(\Lambda)}{d\Lambda} = -\int_{S_u}^{S_v} \frac{\beta s - q}{(\Lambda - \delta s)^2} ds = -(S_v - S_u)\frac{\frac{\beta\Lambda}{\delta} - q}{(\Lambda - \delta S_v)(\Lambda - \delta S_u)} + \frac{\beta}{\delta^2}\ln\left(\frac{-\delta S_u + \Lambda}{-\delta S_v + \Lambda}\right)$$

and $\lim_{\Lambda \to +\infty} \frac{dJ_{12}(\Lambda)}{d\Lambda} = 0$. Moreover, we have

$$\frac{dJ_{12}^2(\Lambda)}{d\Lambda^2} = \int_{S_u}^{S_v} \frac{2(\beta s - q)}{(\Lambda - \delta s)^3} ds = -\frac{\beta(S_u - S_v)\left[(S_u + S_v - 2S^*)\Lambda - (2S_u S_v - S^*(S_u + S_v))\delta\right]}{(-S_v\delta + \Lambda)^2(-S_u\delta + \Lambda)^2}$$

If $S^* = \frac{S_v + S_u}{2}$, then we have $\frac{2}{\frac{1}{S_v} + \frac{1}{S_u}} < S^*$ and

$$\frac{dJ_{12}^2(\Lambda)}{d\Lambda^2} = \int_{S_u}^{S_v} \frac{2(\beta s - q)}{(\Lambda - \delta s)^3} ds = \frac{\beta(S_v - S_u)\left[-\left(\frac{2}{\frac{1}{S_v} + \frac{1}{S_u}} - S^*\right)(S_u + S_v)\delta\right]}{(-S_v\delta + \Lambda)^2(-S_u\delta + \Lambda)^2} > 0$$

which indicates that $\frac{dJ_{12}(\Lambda)}{d\Lambda}$ is monotonically increasing on the interval $(S_v\delta, +\infty)$. Moreover, it follows from $\lim_{\Lambda \to +\infty} \frac{dJ_{12}(\Lambda)}{d\Lambda} = 0$ that $\frac{dJ_{12}(\Lambda)}{d\Lambda} < 0$ for all $\Lambda \in (S_v\delta, +\infty)$, i.e., $J_{12}(\Lambda)$ is monotonically decreasing on the interval $(S_v\delta, +\infty)$. All these results confirm that $J_{12}(\Lambda) > 0$ (i.e., $R_c(\Lambda) > 1$) for all $\Lambda \in (\delta S_v, +\infty)$, which means that the DFPS is unstable and no bifurcation occurs with respect to Λ. If $S^* \neq \frac{S_v + S_u}{2}$, then solving $\frac{dJ_{12}^2(\Lambda)}{d\Lambda^2} = 0$ yields $\tilde{\Lambda} = \delta(\frac{\frac{2S_vS_u}{S_v+S_u} - S^*}{(\frac{S_u+S_v}{2} - S^*)\frac{2}{S_v+S_u}})$. For the bifurcation related to the parameter Λ, we consider the following cases:

(i) If $\frac{S_v+S_u}{2} > \frac{2}{\frac{1}{S_v}+\frac{1}{S_u}} > S^*$ then we have $\tilde{\Lambda} > 0$.

(a) For this case, we first consider $\tilde{\Lambda} > \delta S_v$, and we have $\frac{dJ_{12}^2(\Lambda)}{d\Lambda^2} < 0$ for $\Lambda \in (\delta S_v, \tilde{\Lambda}]$; $\frac{dJ_{12}^2(\Lambda)}{d\Lambda^2} \geq 0$ for all $\Lambda \in [\tilde{\Lambda}, +\infty)$. Correspondingly, the function $\frac{dJ_{12}(\Lambda)}{d\Lambda}$ is monotonically decreasing on the interval $(\delta S_v, \tilde{\Lambda}]$ and monotonically increasing on the interval $[\tilde{\Lambda}, +\infty)$. Moreover, $\lim_{\Lambda \to +\infty} \frac{dJ_{12}(\Lambda)}{d\Lambda} = 0$; thus, we have $\frac{dJ_{12}(\Lambda)}{d\Lambda} < 0$ for all $\Lambda \in [\tilde{\Lambda}, +\infty)$. Now, we claim that $\frac{dJ_{12}(\Lambda)}{d\Lambda} < 0$ for all $\Lambda \in (\delta S_v, \tilde{\Lambda}]$. Otherwise, we assume that there exists a unique $\hat{\Lambda} \in (\delta S_v, \tilde{\Lambda})$ such that $\frac{dJ_{12}(\hat{\Lambda})}{d\Lambda} = 0$, then we have $\frac{dJ_{12}(\Lambda)}{d\Lambda} \geq 0$ for all $\Lambda \in (\delta S_v, \hat{\Lambda}]$ and $\frac{dJ_{12}(\Lambda)}{d\Lambda} < 0$ for all $\Lambda \in (\hat{\Lambda}, +\infty)$. Consequently, $J_{12}(\Lambda)$ is monotonically increasing on the interval $(\delta S_v, \hat{\Lambda}]$ and decreasing on the interval $(\hat{\Lambda}, +\infty)$, which contradicts $\lim_{\frac{\Lambda}{\delta} \to +\infty} J_{12}(\Lambda) = 0$ and $\lim_{\frac{\Lambda}{\delta} \to S_v} J_{12}(\Lambda) = +\infty$. Therefore, $\frac{dJ_{12}(\Lambda)}{d\Lambda} < 0$ for all $\Lambda \in (\delta S_v, +\infty)$ and $J_{12}(\Lambda)$ is monotonically decreasing on $(S_v\delta, +\infty)$, with $J_{12}(\Lambda) > 0$ for all $\Lambda \in (\delta S_v, +\infty)$. All these results confirm that the DFPS is unstable and the bifurcation does not occur at all for this case.

(b) When $\tilde{\Lambda} \leq \delta S_v$, from which we have $\frac{dJ_{12}^2(\Lambda)}{d\Lambda^2} > 0$ for all $\Lambda \in (\delta S_v, +\infty)$. Thus, $\frac{dJ_{12}(\Lambda)}{d\Lambda}$ is monotonically increasing on the interval $(\delta S_v, +\infty)$ with $\lim_{\Lambda \to +\infty} \frac{dJ_{12}(\Lambda)}{d\Lambda} = 0$, which means that $\frac{dJ_{12}(\Lambda)}{d\Lambda} < 0$ for all $\Lambda \in (S_v\delta, +\infty)$ and $J_{12}(\Lambda)$ is monotonically decreasing on $(S_v\delta, +\infty)$. According to $\lim_{\frac{\Lambda}{\delta} \to +\infty} J_{12}(\Lambda) = 0$, we have $J_{12}(\Lambda) > 0$ for all $\Lambda \in (\delta S_v, +\infty)$ and then $R_c(\Lambda) > 1$ holds true, and again the DFPS is unstable and the bifurcation does not occur at all for this case.

(ii) If $\frac{S_v+S_u}{2} > S^* \geq \frac{2}{\frac{1}{S_v}+\frac{1}{S_u}}$, then $\tilde{\Lambda} < 0$. For this case, we have $\frac{dJ_{12}^2(\Lambda)}{d\Lambda^2} > 0$ for all $\Lambda \in (\delta S_v, +\infty)$. By using methods similar to those in (*b*) we can show that $J_{12}(\Lambda) > 0$ for all $\Lambda \in (\delta S_v, +\infty)$ and $R_c(\Lambda) > 1$, which indicates that no bifurcation occurs at all in such case.

(iii) If $S^* > \frac{S_v+S_u}{2} > \frac{2}{\frac{1}{S_v}+\frac{1}{S_u}}$, then $\tilde{\Lambda} > 0$. Now, we claim that $\tilde{\Lambda} > \delta S_v$. Otherwise, we assume that $\tilde{\Lambda} \leq \delta S_v$, then we have $\frac{dJ_{12}^2(\Lambda)}{d\Lambda^2} < 0$ for all $\Lambda \in (\delta S_v, +\infty)$ and $\frac{dJ_{12}(\Lambda)}{d\Lambda}$ is monotonically decreasing on $(\delta S_v, +\infty)$. Moreover, we have $\lim_{\frac{\Lambda}{\delta} \to +\infty} J_{12}(\Lambda) = 0$, thus $\frac{dJ_{12}(\Lambda)}{d\Lambda} > 0$ for all $\Lambda \in (\delta S_v, +\infty)$, i.e., $J_{12}(\Lambda)$ is monotonically increasing on $(S_v\delta, +\infty)$, which contradicts $\lim_{\frac{\Lambda}{\delta} \to +\infty} J_{12}(\Lambda) = 0$ and $\lim_{\frac{\Lambda}{\delta} \to S_v} J_{12}(\Lambda) = +\infty$.

Thus, $\frac{dJ_{12}^2(\Lambda)}{d\Lambda^2} \geq 0$ for all $\Lambda \in (\delta S_v, \tilde{\Lambda}]$, and $\frac{dJ_{12}^2(\Lambda)}{d\Lambda^2} < 0$ for all $\Lambda \in (\tilde{\Lambda}, +\infty)$. Moreover, according to $\lim_{\Lambda \to +\infty} \frac{dJ_{12}(\Lambda)}{d\Lambda} = 0$ we have $\frac{dJ_{12}(\Lambda)}{d\Lambda} > 0$ for all $\Lambda \in [\tilde{\Lambda}, +\infty)$. It is easy to know that there exists a unique $\hat{\Lambda} \in (\delta S_v, \tilde{\Lambda})$ such that $\frac{dJ_{12}(\hat{\Lambda})}{d\Lambda} = 0$, and $\frac{dJ_{12}(\Lambda)}{d\Lambda} \leq 0$ for all $\Lambda \in (\delta S_v, \hat{\Lambda}]$; $\frac{dJ_{12}(\Lambda)}{d\Lambda} > 0$ for all $\Lambda \in (\hat{\Lambda}, +\infty)$. According to $\lim_{\frac{\Lambda}{\delta} \to +\infty} J_{12}(\Lambda) = 0$ and $\lim_{\frac{\Lambda}{\delta} \to S_v} J_{12}(\Lambda) = +\infty$, we know that there exists a unique $\Lambda^* \in (\delta S_v, \hat{\Lambda})$ such that $J_{12}(\Lambda^*) = 0$, i.e., $R_c(\Lambda^*) = 1$ with $\frac{dJ_{12}(\Lambda^*)}{d\Lambda} < 0$ and $\frac{dR_c(\Lambda^*)}{d\Lambda} < 0$.

By employing methods similar to those above, we can show that $P_M(Y, \Lambda)$ will occur with the bifurcation as $\Lambda = \Lambda^*$ for this case, which depends on the magnitude of M, i.e., if $M \neq \frac{2\eta_2}{h_2}$ then a transcritical bifurcation occurs; if $M = \frac{2\eta_2}{h_2}$ and $\frac{\partial^3 P_M(0,\Lambda^*)}{\partial Y^3} \neq 0$, then a pitchfork bifurcation occurs.

In summary, if $\frac{S_v+S_u}{2} \geq S^*$, then $J_{12}(\Lambda)$ is monotonically decreasing on the interval $(S_v\delta, +\infty)$; if $\frac{S_v+S_u}{2} < S^*$, then $J_{12}(\Lambda)$ is monotonically decreasing on the interval $(\delta S_v, \hat{\Lambda}]$ and increasing on the interval $(\hat{\Lambda}, +\infty)$. Moreover, we have the following main results:

THEOREM 8. *Assume that* $h_2 \neq 0$, $1 < \frac{S_v}{S^*} < R_0$. *If* $\frac{S_v+S_u}{2} \geq S^*$, *then* $J_{12}(\Lambda)$ *is monotonically decreasing on the interval* $(S_v\delta, +\infty)$ *and* $R_c(\Lambda) > 1$ *for all* Λ, *which means that the DFPS* $(S^T(t), 0)$ *is unstable. If* $\frac{S_v+S_u}{2} < S^*$, *then* $J_{12}(\Lambda)$ *is monotonically decreasing on the interval* $(\delta S_v, \hat{\Lambda}]$ *and increasing on the interval* $(\hat{\Lambda}, +\infty)$. *There exists a unique* $\Lambda^* \in (S_v\delta, +\infty)$ *such that* $R_c(\Lambda^*) = 1$ *and* $P_M(Y, \Lambda)$ *occurs with a bifurcation at* $\Lambda = \Lambda^*$. *Moreover, if* $M \neq \frac{2\eta_2}{h_2}$, *then a transcritical bifurcation occurs; if* $M = \frac{2\eta_2}{h_2}$ *and* $\frac{\partial^3 P_M(0,\Lambda^*)}{\partial Y^3} \neq 0$, *then a pitchfork bifurcation occurs.*

In particular, if $h_2 = 0$, we have $R_c(\Lambda) = (1-\eta_2)\exp(J_{12}(\Lambda))$ with $\lim_{K\to+\infty} J_{12}(\Lambda) = 0$ and $\lim_{K\to S_v} J_{12}(\Lambda) = +\infty$, which indicate that there exists a unique $\Lambda^* \in (S_v\delta, +\infty)$ such that $J_{12}(\Lambda^*) = \ln\frac{1}{1-\eta_2} > 0$, i.e., $R_c(\Lambda^*) = 1$ with $\frac{dJ_{12}(\Lambda^*)}{d\Lambda} < 0$. Based on the monotonicity of $J_{12}(\Lambda)$, we conclude that no matter what the relationship between $\frac{S_v+S_u}{2}$ and S^*, critical value Λ^* exists and is unique. Moreover, according to $\frac{\partial^2 P_M(0,\Lambda^*)}{\partial Y^2} = M > 0$, we have the following main results:

COROLLARY 5. *If* $h_2 = 0$, $1 < \frac{S_v}{S^*} < R_0$, *then* $P_M(Y, \Lambda)$ *occurs with the transcritical bifurcation at* $\Lambda = \Lambda^*$, *which indicates that an unstable positive fixed point of the* $P_M(Y, \Lambda)$ *appears when the parameter* Λ *changes through* Λ^* *from left to right. Correspondingly, system (2) has an unstable positive periodic solution if* $\Lambda \in (\Lambda^*, \Lambda^* + \epsilon)$ *with* $\epsilon > 0$ *small enough.*

Note that if $h_2 = 0$ and $P_M(Y)$ occurs with bifurcations with respect to parameters η_1, η_2, S_v, Λ, then we must have

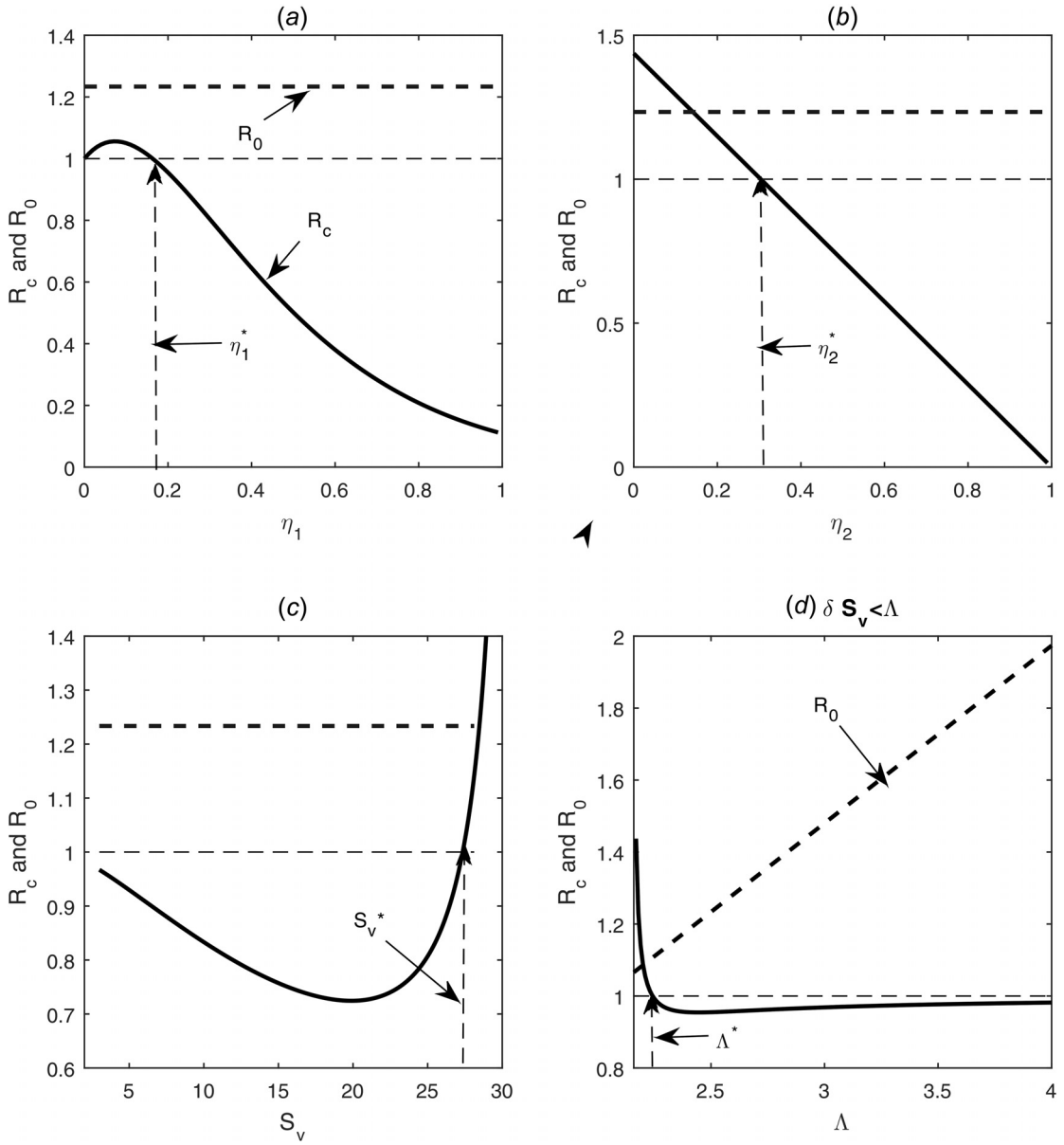

Fig. 3 The existence of threshold parameter values for transcritical bifurcations for $\eta_1^*, \eta_2^*, S_v^*, \Lambda^*$. The base line parameter values are as follows: $\Lambda = 2.5$, $\beta = 0.015$, $\delta = 0.08$, $\gamma = 0.3$, $h_1 = 5$, $\eta_1 = 0.2$, $\eta_2 = 0.1$, $h_2 = 3$, and $S_v = 27$ in (*a*), (*d*) and 29 in (*b*) with $h_2 = 0$.

$\frac{\partial^2 P_M(0,\eta_1^*)}{\partial Y^2} = \frac{\partial^2 P_M(0,\eta_2^*)}{\partial Y^2} = \frac{\partial^2 P_M(0,S_v^*)}{\partial Y^2} = \frac{\partial^2 P_M(0,\Lambda^*)}{\partial Y^2} = M > 0$. Thus, we conclude that:

THEOREM 9. *If $h_2 = 0$ and $P_M(Y)$ occurs with a bifurcation with respect to the parameters η_1, η_2, S_v, Λ, then it must be a transcritical bifurcation and generates an unstable interior periodic solution, i.e., a backward bifurcation occurs and bistability appears when the DFPS of model (2) and the interior equilibrium $P^*(S^*, I^*)$ can coexist.*

5 Discussion

The basic or control reproduction number plays a key role in analyzing dynamics of epidemic models, but how to define and calculate it is challenging due to the complexity of the various control measures involved in the models. In particular, most control measures are implemented instantaneously, which can be modeled by impulsive differential equations with fixed or unfixed moments. Infectious disease models with pulse vaccination or treatment strategies have been widely studied recently [5,7,8,10,13,15,19,20], and most of the models assume that the pulse vaccination or treatment tactics occurs at a fixed period (i.e., fixed moment) resulting in nonautonomous periodic systems. If so, we cannot employ the theories of dynamic systems, especially the theories of impulsive dynamical systems, to study the dynamic behavior of the model, and then to determine the threshold dynamic behavior and bifurcation phenomenon of the proposed model. Therefore, in order to overcome the above shortcomings, in the present paper, we have extended the classic SIR model of infections by involving state-dependent feedback control guided by a threshold size of the susceptible population, aiming to address the threshold dynamics and determine the threshold condition through the bifurcation theories of the discrete one-parameter family of maps.

The existence and global stability of the DFPS, which corresponds to the disease-free equilibrium of the model without control actions, have been investigated in detail, and the main results show that $R_0 \leq 1$ indicates $R_c < 1$, which reveals that the nonexistence of the interior equilibrium for the classical SIR model (1) implies the existence and global stability of the DFPS $(S^T(t), 0)$. Moreover, if $R_0 > 1$, we conclude that the disease can still be completely eradicated provided that a proper choice of the threshold susceptible population size S_v is made, i.e., if we choose the threshold level $S_v < S^*$, then the DFPS $(S^T(t), 0)$ could be globally stable even if $R_0 > 1$ for the SIR model (1). All these results confirm that state-dependent feedback control can be effectively used for mitigating and eradicating infectious diseases [7,8,11–14].

The control reproduction number R_c for model (2) could be defined based on the threshold condition for the stability of the DFPS $(S^T(t), 0)$. Further, the bifurcation analyses of the discrete one-parameter family of maps, which is determined by the Poincaré map of the proposed model (2), related to all interesting parameters of model (2) confirm that R_c can determine the threshold dynamics of model (2). In particular, the super-critical or subcritical transcritical and pitchfork bifurcations related to the maximal vaccination rate η_1, treatment or isolation rate η_2, threshold size S_v and model parameter Λ have been shown when we assume that the Poincaré map P_M is well defined in the neighborhood of $U(0^+)$.

In fact, the Poincaré map $P_M(Y)$ is well defined for all small Y shown in Fig. 2(*d*). Moreover, it can be confirmed from the properties of the phase portrait of model (1). It follows from $S_v > S^*$ that there exists a unique trajectory Γ_2 of model (1), which tangents to the line $S = S_v$ (i.e., l_3) at the point $A = (S_v, I_A)$, and intersects with the line $l_4(S = S_u)$ at the point $C(S_u, I_c)$ with $I_A = \frac{-\delta S_v + \Lambda}{\beta S_v}$. Therefore, $P_M(Y)$ is well defined on the domain $[0, I_c]$ with range $[0, f(I_A)]$. However, since the sign of $\frac{\partial^2 P_M(Y)}{\partial Y^2}$ on the interval $[0, I_c]$ varies as parameters change, we cannot determine the convexity and concavity of $P_M(Y)$, which presents a major challenge when addressing the existence and stability of the order-1 periodic solution by using the properties of the Poincaré map $P_M(Y)$.

The existence of threshold parameter values of $\eta_1^*, \eta_2^*, S_v^*, \Lambda^*$ for transcritical bifurcations and backward bifurcations is shown in Fig. 3, which further confirms that the four interesting parameters chosen for bifurcation analyses can be well defined. Meanwhile, the unstable interior order-1 periodic solution could bifurcate from the DFPS through the transcritical bifurcation, i.e., the backward bifurcation occurs, and consequently the stable DFPS of model (2) and equilibrium P^* of model (1) could coexist. Note that it follows from the main Theorems in Sec. 4 that the necessary conditions for the occurrences of the backward bifurcations are $R_c < 1 < R_0$ and $S_v > S^*$, which show that the disease will have outbreaks when the control measures are not involved (i.e., the global stability of P^* of model (1)). Once the control measures are involved in the model, we conclude that the disease can be controlled even if the threshold level is relatively large ($S_v > S^*$ here). Furthermore, the necessary condition $R_c < 1 < R_0$ for the occurrence of a backward bifurcation implies that there must exist a threshold value $\bar{R}_c$ such that the DFPS is globally stable for $R_c < \bar{R}_c$, and the stable DFPS of model (2) and equilibrium P^* of model (1) could coexist $\bar{R}_c < R_c < 1 < R_0$. An interesting question is how to analytically determine the threshold value $\bar{R}_c$, a challenge for future work.

Moreover, the relations between R_c and R_0 for the four interesting parameters shown in Figs. 1(*a*), 1(*c*), and 3 reveal that no matter whether the R_0 is greater than or less than 1, there is a certain parameter space that makes R_c greater than R_0. The results shown in Fig. 1(*a*) confirm that the implementation of integrated control measures is not conducive to the elimination of disease when the control threshold level S_v is less than the critical value $\bar{S}_v$, and the results shown in Fig. 1(*c*) show the importance of selecting the threshold level S_v for infectious disease control. Moreover, the results presented in Fig. 3 provide an important way of thinking about how to control infectious diseases. For example, if $-\frac{\beta}{\delta}(S_v - S^*) + \frac{1}{\delta}(\beta K - q) \ln(\frac{K - S^*}{K - S_v}) > \ln R_0$, i.e., $R_c(\bar{\eta}_1) > R_0$, then $R_c(\eta_1) > R_0$ for $\eta_1 \in U(\bar{\eta}_1, \delta)$ (i.e., the δ domain of $\bar{\eta}_1$). Numerical simulations reveal that this phenomenon occurs only when the maximal vaccination η_1 is very small, as shown in Fig. 3(*a*). Note that the biphasic vaccination rate results in an inverted U-shape curve for η_1 shown in Fig. 3(*a*), i.e., too low a vaccination rate increases the R_c and a relatively high vaccination rate decreases the R_c. All these results confirm that increasing vaccination coverage is very important in controlling infectious diseases, especially when the implementation of the vaccination strategy depends on the size of the susceptible population.

Similarly, the biphasic threshold level S_v results in a U-shape curve shown in Fig. 3(*c*), i.e., too small or too large a threshold level S_v is not beneficial for disease control. Moreover, R_c could be larger than R_0 provided that the S_v is large enough, which can be confirmed as follows: it follows from $\lim_{S_v \to S^*} J_{12}(S_v) < 0$, $\lim_{S_v \to K} J_{12}(S_v) = +\infty$ and the continuity of $J_{12}(S_v)$ that there exists a $S_{v0} \in (S^*, K)$ such that $J_{12}(S_{v0}) = \ln R_0 > 0$ (i.e., $R_c(S_{v0}) = R_0$), and $R_c(S_{v0}) > R_0$ for all $S_v \in (S_{v0}, K)$. Moreover, the line $S_v = K$ is an asymptote of $R_c(S_v)$. Thus, we conclude that the U-shape curve related to the S_v reveals the importance of the correct selection of the threshold level to ensure the best integrated disease control effect. Note that biphasic dose response curves have been reported in many areas recently, including cancer treatment and pest control [39–41], but this is the first time that we have found that biphasic vaccination and threshold size responses occur in an infectious disease model with state-dependent feedback control. In order to eradicate infectious diseases, the size of the susceptible population (i.e., the critical level S_v here) plays a key role, which provides important ideas and guidance for designing vaccine output and coverage according to population size and vaccine effectiveness.

The results shown in Fig. 3(*b*) clarify that only high rates of effective treatment or isolation could successfully mitigate or eradicate the infectious disease. The birth rate Λ could also influence the R_c significantly, as shown in Fig. 3(*d*). For the parameter values given in Fig. 3(*d*) we have $\frac{S_v+S_u}{2} = 24.72 < S^*$, where $S^* = 25.33$, $S_u = 22.44$ and the results correspond to Theorem 8. In particular, if $\eta_1 \leq \frac{2(S_v+h_1)(1-\frac{S^*}{S_v})}{S_v} \doteq 0.147$, then $R_c(\Lambda)$ is monotonically decreasing on the interval $[\delta S_v, \infty)$ and tends to 1; if $\eta_1 > \frac{2(S_v+h_1)(1-\frac{S^*}{S_v})}{S_v} \doteq 0.147$, then $R_c(\Lambda)$ is monotonically decreasing first and then increasing on the interval $[\delta S_v, \infty)$, which will tend to 1 eventually, and this is the case shown in Fig. 3(*d*). The relations between η_1 and $\frac{2(S_v+h_1)(1-\frac{S^*}{S_v})}{S_v}$ clearly reveal that how to design the vaccination campaign (i.e., choosing the vaccination rate η_1) should be based on the threshold size S_v and stable population level S^* without control measures. Also, the results shown in Fig. 3(*d*) demonstrate that for a relatively large birth rate Λ, we must choose a high vaccination rate η_1 such that $R_c < 1$. In conclusion, in order to effectively control the outbreak of infectious diseases, we should take effective, timely, measures that are stronger than usual, including vaccination, treatment, and isolation, which should be adopted in relation to monitored population births and growth.

The properties of the function $f(I) = 1 - \frac{\eta_1 I(t)}{I(t)+h_2}$ can significantly affect the monotonicity and concavity of the Poincaré map P_M, which will result in the complexity of the P_M, and consequently various different methods have been developed in the present paper to show the global stability of DFPS by considering nonlinear impulsive perturbations have in comparison with the results obtained in Ref. [38]. Moreover, it is interesting to note that the control reproduction number $R_c = (1-\eta_2)\exp(J_2 + J_3)$ for $h_2 = 0$, which indicates that the nonlinear pulse perturbation can significantly affect R_c and consequently influences the bifurcation of $P_M(Y)$. In particular, $P_M(Y)$ could only occur with a transcritical bifurcation when $h_2 = 0$, and the pitchfork bifurcation could occur when $h_2 > 0$. Further, the Poincare map $P_M(Y, \eta_1)$ can occur with a transcritical bifurcation at $\eta_1 = \eta_1^*$ when $h_2 > 0$, i.e., there exists a unique bifurcation value η_1^* when the nonlinear pulse is considered, while there may exist two bifurcation values once $h_2 = 0$.

Therefore, we conclude that the nonlinear impulsive perturbations addressed in the present paper are not only more practical and can produce rich dynamic behavior, but also required new analytical techniques and methods to investigate their global dynamic behavior. The idealized hypothesis proposed allowed us to simplify our model and thus conduct a thorough theoretical analysis, but undeniably it led to limitations to the application of our model to real events. Thus, we leave the interesting question of how to apply our new methods and techniques to a more general model for our future research.

Funding Data

- National Natural Science Foundation of China (NSFCs) (61772017 and 11631012; Funder ID: 10.13039/501100001809).
- Fundamental Research Funds for the Central Universities (GK201901008; Funder ID: 10.13039/501100002338).

Appendix

The following lemma shows the local stability of the T-periodic solution of the plane impulsive semidynamical system.

LEMMA A.1. *The T-periodic solution $(x, y) = (\xi(t), \eta(t))$ of the system*

$$\begin{cases} \left.\begin{aligned} \frac{dx(t)}{dt} &= P(x,y), \\ \frac{dy(t)}{dt} &= Q(x,y), \end{aligned}\right\} & \text{if } \phi(x,y) \neq 0 \\ \left.\begin{aligned} \triangle x &= \sigma_1(x,y), \\ \Delta y &= \sigma_2(x,y), \end{aligned}\right\} & \text{if } \phi(x,y) = 0 \end{cases} \tag{A1}$$

is orbitally asymptotically stable if the Floquet multiplier μ_2 satisfies the condition $|\mu_2| < 1$, where

$$\mu_2 = \prod_{k=1}^{q} \triangle_k \exp\left[\int_0^T \left(\frac{\partial P}{\partial x}(\xi(t),\eta(t)) + \frac{\partial Q}{\partial y}(\xi(t),\eta(t))\right) dt\right] \tag{A2}$$

with

$$\Delta_k = \frac{P_+\left(\frac{\partial \sigma_2}{\partial y}\frac{\partial \phi}{\partial x} - \frac{\partial \sigma_2}{\partial x}\frac{\partial \phi}{\partial y} + \frac{\partial \phi}{\partial x}\right) + Q_+\left(\frac{\partial \sigma_1}{\partial x}\frac{\partial \phi}{\partial y} - \frac{\partial \sigma_1}{\partial y}\frac{\partial \phi}{\partial x} + \frac{\partial \phi}{\partial y}\right)}{P\frac{\partial \phi}{\partial x} + Q\frac{\partial \phi}{\partial y}}$$

and P, Q, $\frac{\partial \sigma_1}{\partial x}$, $\frac{\partial \sigma_1}{\partial y}$, $\frac{\partial \sigma_2}{\partial x}$, $\frac{\partial \sigma_2}{\partial y}$, $\frac{\partial \phi}{\partial x}$, and $\frac{\partial \phi}{\partial y}$ are calculated at the point $(\xi(t), \eta(t))$. $P_+ = P(\xi(t_k^+), \eta(t_k^+))$ and $Q_+ = Q(\xi(t_k^+), \eta(t_k^+))$. Here, $\phi(x, y)$ is a sufficiently smooth function such that grad $\phi(x, y) \neq 0$, and $t_k (k \in N)$ is the time of the kth jump.

The following two lemmas show the transcritical and pitchfork bifurcations of the discrete one-parameter family of maps, which can be used to address the stability and bifurcation of the Poincaré map determined by the impulsive point series of the impulsive semidynamical system.

LEMMA A.2. *(Transcritical bifurcation) Let $G: U \times I \to R$ define a one-parameter family of maps, where G is C^r with $r \geq 2$, and U, I are open intervals of the real line containing 0. Assume that*

(1) $G(0, \alpha) = 0$ *for all* α;
(2) $\frac{\partial G}{\partial x}(0,0) = 1$;
(3) $\frac{\partial^2 G}{\partial x \partial \alpha}(0,0) > 0$;
(4) $\frac{\partial^2 G}{\partial^2 x}(0,0) > 0$.

Then, there are $\alpha_1 < 0 < \alpha_2$ and $\varepsilon > 0$ such that

(i) *If $\alpha_1 < \alpha < 0$, then $G_\alpha = G(.,\alpha)$ has two fixed points, 0 and $x_{1\alpha} > 0$ in $(-\varepsilon, \varepsilon)$, then the origin is asymptotically stable and the other fixed point is unstable.*
(ii) *If $0 < \alpha < \alpha_2$, then G_α has two fixed points, 0 and $x_{1\alpha} < 0$ in $(-\varepsilon, \varepsilon)$. The origin is unstable, the other fixed point is asymptotically stable.*

Note that the case $\frac{\partial^2 G}{\partial x \partial \alpha}(0,0) < 0$ is handled by making the change of parameter $\alpha \to -\alpha$. If the inequality (4) is reversed (i.e., $\frac{\partial^2 G}{\partial^2 x}(0,0) < 0$), then

(i) *If $\alpha_1 < \alpha < 0$, then G_α has two fixed points, 0 and $x_{1\alpha} < 0$ in $(-\varepsilon, \varepsilon)$. The origin is asymptotically stable, the other fixed point is unstable.*
(ii) *If $0 < \alpha < \alpha_2$, then G_α has two fixed points, 0 and $x_{1\alpha} > 0$ in $(-\varepsilon, \varepsilon)$. The origin is unstable, and the other fixed point is asymptotically stable.*

LEMMA A.3. *(Supercritical pitchfork bifurcation) Let* $G: U \times I \to R$ *be as in Lemma A.2, except that* G *is* C^r *with* $r \geq 3$ *and* $\frac{\partial^2 G}{\partial x^2}(0,0) = 0$. *Further, if* $\frac{\partial^3 G}{\partial x^3}(0,0) < 0$ *then there are* $\alpha_1 < 0 < \alpha_2$ *and* $\varepsilon > 0$ *such that*

(i) *If* $\alpha_1 < \alpha \leq 0$, *then* $G_\alpha = G(., \alpha)$ *has a unique fixed point,* $x = 0$, *in* $(-\varepsilon, \varepsilon)$. *It is asymptotically stable.*
(ii) *If* $0 < \alpha < \alpha_2$, *then* G_α *has three fixed points in* $(-\varepsilon, \varepsilon)$. *The origin is an unstable fixed point, the two others,* $x_{1\alpha} < 0 < x_{2\alpha}$, *are asymptotically stable.*

Note that the case $\frac{\partial^2 G}{\partial x \partial \alpha}(0,0) < 0$ *is identical to the above after the change of parameter* $\alpha \to -\alpha$. *If* $\frac{\partial^3 G}{\partial x^3}(0,0) > 0$, *it is a so-called subcritical pitchfork bifurcation. Then for* $\alpha < 0$, *there are three fixed points near the origin, but only* $x = 0$ *is asymptotically stable. For* $\alpha \geq 0$, *the origin is the unique fixed point near* $x = 0$, *and it is unstable.*

References

[1] Ferguson, N. M., Cummings, D. A. T., Cauchemez, S., Fraser, C., Riley, S., Meeyai, A., Iamsirithaworn, S., and Burke, D. S., 2005, "Strategies for Containing an Emerging Influenza Pandemic in Southeast Asia," Nature, **437**(7056), pp. 209–214.
[2] Fraser, C., Donnelly, C. A., Cauchemez, S., Hanage, W. P., Van Kerkhove, M. D., Hollingsworth, T. D., Griffin, J., Baggaley, R. F., Jenkins, H. E., Lyons, E. J., Jombart, T., Hinsley, W. R., Grassly, N. C., Balloux, F., Ghani, A. C., Ferguson, N. M., Rambaut, A., Pybus, O. G., Lopez-Gatell, H., Alpuche-Aranda, C. M., Chapela, I. B., Zavala, E. P., Guevara, D. M. E., Checchi, F., Garcia, E., Hugonnet, S., and Roth, C., 2009, "Pandemic Potential of a Strain of Influenza A (H1N1): Early Findings," Science, **324**(5934), pp. 1557–1561.
[3] Tang, S. Y., Xiao, Y. N., Yuan, L., Cheke, R. A., and Wu, J. H., 2012, "Campus Quarantine (Fengxiao) for Curbing Emergent Infectious Diseases: Lessons From Mitigating a/H1N1 in Xi'an, China," J. Theor. Biol., **295**, pp. 47–58.
[4] Xiao, Y. N., Tang, S. Y., and Wu, J. H., 2015, "Media Impact Switching Surface During an Infectious Disease Outbreak," Sci. Rep., **5**, p. 7838.
[5] Agur, Z., Cojocaru, L., Mazor, G., Anderson, R. M., and Danon, Y. L., 1993, "Pulse Mass Measles Vaccination Across Age Cohorts," Proc. Natl. Acad. Sci. U. S. A., **90**(24), pp. 11698–11702.
[6] Mailleret, L., and Lemesle, V., 2009, "A Note on Semi-Discrete Modelling in the Life Sciences," Phil. Trans. R. Soc., A, **367**(1908), pp. 4779–4799.
[7] Shulgin, B., Stone, L., and Agur, Z., 1998, "Pulse Vaccination Strategy in the SIR Epidemic Model," Bull. Math. Biol., **60**(6), pp. 1123–1148.
[8] Fuhrman, K. M., Lauko, I. G., and Pinter, G. A., 2004, "Asymptotic Behavior of an SI Epidemic Model With Pulse Removal," Math. Comput. Model., **40**(3–4), pp. 371–386.
[9] Gao, S. J., Chen, L., Nieto, J. J., and Torres, A., 2006, "Analysis of a Delayed Epidemic Model With Pulse Vaccination and Saturation Incidence," Vaccine, **24**(35–36), pp. 6037–6045.
[10] Gao, S. J., Chen, L. S., and Teng, Z. D., 2007, "Impulsive Vaccination of an SEIRS Model With Time Delay and Varying Total Population Size," Bull. Math. Biol., **69**(2), pp. 731–745.
[11] Liu, X. N., Takeuchi, Y., and Iwami, S., 2008, "SVIR Epidemic Models With Vaccination Strategies," J. Theor. Biol., **253**(1), pp. 1–11.
[12] Meng, X. Z., and Chen, L. S., 2008, "The Dynamics of a New SIR Epidemic Model Concerning Pulse Vaccination Strategy," Appl. Math. Comput., **197**(2), pp. 582–597.
[13] D'Onofrio, A., 2002, "Stability Properties of Pulse Vaccination Strategy in SEIR Epidemic Model," Math. Biosci., **179**, pp. 57–72.
[14] D'Onofrio, A., 2005, "On Pulse Vaccination Strategy in the SIR Epidemic Model With Vertical Transmission," Appl. Math. Lett., **18**, pp. 729–732.
[15] Lakmeche, A., and Arino, O., 2000, "Bifurcation of Non-Trivial Periodic Solutions of Impulsive Differential Equations Arising Chemotherapeutic Treatment," Dyn. Contin. Discrete Impulsive Syst., **7**, pp. 265–287.
[16] Lakmeche, A., and Arino, O., 2001, "Nonlinear Mathematical Model of Pulsed-Therapy of Heterogeneous Tumors," Nonlinear Anal.: Real World Appl., **2**, pp. 455–465.
[17] Panetta, J. C., 1996, "A Mathematical Model of Periodically Pulsed Chemotherapy: Tumor Recurrence and Metastasis in a Competitive Environment," Bull. Math. Biol., **58**(3), pp. 425–447.
[18] Panetta, J. C., 1998, "A Mathematical Model of Drug Resistance: Heterogeneous Tumors," Math. Biosci., **147**(1), pp. 41–61.
[19] Bunimovich-Mendrazitsky, S., Byrne, H., and Stone, L., 2008, "Mathematical Model of Pulsed Immunotherapy for Superficial Bladder Cancer," Bull. Math. Biol., **70**(7), pp. 2055–2076.
[20] Liu, M. X., and Jin, Z., 2006, "The Effect of Impulsive Control Strategy in HIV/AIDS Model," Dyn. Contin. Discrete Ser., A, **13**, pp. 706–713.
[21] Smith, R. J., and Schwartz, E. J., 2008, "Predicting the Potential Impact of a Cytotoxic T-Lymphocyte HIV Vaccine: How Often Should You Vaccinate and How Strong Should the Vaccine Be?," Math. Biosci., **212**(2), pp. 180–187.
[22] Bainov, D. D., and Simeonov, P. S., 1989, *Systems With Impulsive Effect: Stability, Theory and Applications*, Wiley, New York.
[23] Benchohra, M., Henderson, J., and Ntouyas, S., 2006, *Impulsive Differential Equations and Inclusions*, Hindawi Publishing Corporation, New York.
[24] Kaul, S. K., 1990, "On Impulsive Semidynamical Systems," J. Math. Anal. Appl., **150**(1), pp. 120–128.
[25] Kaul, S. K., 1992, "On Impulsive Semidynamical Systems—III: Lyapunov Stability," *Recent Trends in Differential Equations*, World Scientific, London, pp. 335–345.
[26] Kaul, S. K., 1994, "Stability and Asymptotic Stability in Impulsive Semidynamical Systems," J. Appl. Math. Stochastic Anal., **7**(4), pp. 509–523.
[27] Tang, S. Y., and Cheke, R. A., 2005, "Stage-Dependent Impulsive Models of Integrated Pest Management (IPM) Strategies and Their Dynamic Consequences," J. Math. Biol., **50**(3), pp. 257–292.
[28] Tang, S. Y., Xiao, Y. N., Chen, L. S., and Cheke, R. A., 2005, "Integrated Pest Management Models and Their Dynamical Behaviour," Bull. Math. Biol., **67**(1), pp. 115–135.
[29] Tang, S. Y., Pang, W. H., Cheke, R. A., and Wu, J. H., 2015, "Global Dynamics of a State-Dependent Feedback Control System," Adv. Differ. Equations., **2015**, p. 322
[30] Tang, S. Y., Tang, B., Wang, A. L., and Xiao, Y. N., "Holling II Predator-Prey Impulsive Semi-Dynamic Model With Complex Poincare Map," Nonlinear Dyn., **81**(3), pp. 1575–1596.
[31] Tang, S. Y., and Pang, W. H., 2017, "On the Continuity of the Function Describing the Times of Meeting Impulsive Set and Its Application," Math. Biosci. Eng., **14**(5–6), pp. 1399–1406.
[32] Liang, J. H., Tang, S. Y., Nieto, J. J., and Cheke, R. A., 2013, "Analytical Methods for Detecting Pesticide Switches With Evolution of Pesticide Resistance," Math. Biosci., **245**(2), pp. 249–257.
[33] Nie, L. F., Teng, Z. D., and Hu, L., 2011, "The Dynamics of a Chemostat Model With State Dependent Impulsive Effects," Int. J. Bifurcation Chaos, **21**(5), pp. 1311–1322.
[34] Tang, S. Y., and Chen, L. S., 2004, "Modeling and Analysis of Integrated Pest Management Strategy," Discrete Contin. Dyn. Syst., B, **4**, pp. 759–768.
[35] Tang, S. Y., and Cheke, R. A., 2008, "Models for Integrated Pest Control and Their Biological Implications," Math. Biosci., **215**(1), pp. 115–125.
[36] Tang, S. Y., Xiao, Y. N., and Cheke, R. A., 2008, "Multiple Attractors of Host-Parasitoid Models With Integrated Pest Management Strategies: Eradication, Persistence and Outbreak," Theor. Popul. Biol., **73**(2), pp. 181–197.
[37] Tang, S. Y., Liang, J. H., Tan, Y. S., and Cheke, R. A., 2013, "Threshold Conditions for Integrated Pest Management Models With Pesticides That Have Residual Effects," J. Math. Biol., **66**(1–2), pp. 1–35.
[38] Zhang, Q., Tang, B., and Tang, S. Y., 2018, "Vaccination Threshold Size and Backward Bifurcation of SIR Model With State-Dependent Pulse Control," J. Theor. Biol., **455**, pp. 75–85.
[39] Calabrese, E. J., and Edward, J., 2002, "Hormesis: Changing View of the Dose-Response, a Personal Account of the History and Current Status," Mutat. Res., **511**(3), pp. 181–189.
[40] Calabrese, E. J., and Baldwin, L. A., 2003, "Toxicology Rethinks Its Central Belief," Nature, **421**(6924), pp. 691–692.
[41] Pearce, O. M. T., Laubli, H., Verhagen, A., Secrest, P., Zhang, J., Varki, N. M., Crocker, P. R., Bui, J. D., and Varki, A., 2014, "Inverse Hormesis of Cancer Growth Mediated by Narrow Ranges of Tumor-Directed Antibodies," Proc. Natl. Acad. Sci. U. S. A., **111**(16), pp. 5998–6003.